DOI: 10.1002/ejic.200701321

# Rock around the Ring: An Experimental and Theoretical Study of the Molecular Dynamics of Stannyltriphospholes with Chiral Tin Substituents

**Martin Hofmann,[a] Tim Clark,[b] Frank W. Heinemann,[a] and Ulrich Zenneck*[a]**

**Keywords:** Phosphorus heterocycles / Tin / Stereochemistry / Molecular dynamics / Density functional calculations

The reaction of diphenyltin dichloride with enantiopure Grignard reagents prepared in situ leads to diphenyltin chlorides **7a**–**e**, which contain chiral organyl substituents. The 2-bornyl derivative **7a** forms a mixture of *exo* and *endo* isomers and the (–)-menthyl derivative **7b** yields a mixture of epimers, whereas the *cis*- and *trans*-myrtanyl complexes **7c** and **7d** and the *m*-(2-bornyl-2-ene)phenyl species **7e** form only one enantiomer as the tin atom is separated from the next stereogenic centre by a methylene or *m*-phenylene group. The target chirally modified 1-(triorganylstannyl)-1,2,4-triphospholes **2a**–**e** are accessible from **7a**–**e** by treatment of the latter with the salt (3,5-di-*tert*-butyl-1,2,4-triphospholyl)-sodium (Na**5**) in good yield. As for **7c**–**e**, complexes **2c**–**e** exhibit enantiopure organyl tin substituents that combine with the planar chiral 1,2,4-triphosphole moiety to form diastereomers. X-ray diffraction studies on crystalline phases of **2a**,**b**,**d** and **7b**,**c** confirm the stereochemical interpretations of their spectroscopic data with the help of absolute structure parameter determinations. Dynamic NMR spectroscopy experiments with these compounds demonstrate for the first time a facile stannyl group shift between the two adjacent P atoms (P1 and P2) of the heterocycles that includes ring inversion through a planar transition state ($\mathbf{T_i}$). In line with the NMR spectroscopic results for **2a**–**e**, density functional calculations with the simplified model compound (trimethylstannyl)-1,2,4-triphosphole (**9**) point to 1-(trimethylstannyl)-1,2,4-triphosphole (**9a**) as the global energetic minimum for **9** and an almost isoenergetic 1,2-shift and ring inversion as the main epimerisation processes of the two enantiomers of **9a**.



## Introduction

The fluxional behaviour of cyclopentadiene and its derivatives has been a subject of interest for several groups since 1970.[1–3] A similar dynamic molecular behaviour can be observed when one or more of the CH fragments of cyclopentadiene are replaced by isolobal phosphorus atoms to form mono-, di-, tri- or tetraphospholes.[4–6] If a $\lambda^3$-phosphorus atom of a phosphole is bonded to a metallic group 14 or another p-block element, a diene-like character of the five-membered heterocycle results because of the covalent character of the P–M bond.[7,8] As the dynamic behaviour of phospholes involves reversible forming and breaking of P–M and probably of C–M bonds, it also reveals details of the bonding situation in the heterocycles. A facile [1,5]-sigmatropic shift has been observed by dynamic NMR spectroscopy for the $SnPh_3$ group of 1-(triphenylstannyl)-1,2,4-triphosphole (**1**), for example (Figure 1), although the symmetry of the exchange process means that the experimental data do not indicate whether the tin always stays on the same side of the ring or if it also moves to the other side.[7] In the former the stannyl group would oscillate between the two adjacent phosphorus atoms like a windscreen wiper, whereas in the latter it rocks around the $P_2$ edge of **1** or maybe even around the complete π-system of the molecule. Besides simply shifting the substituent to the other P atom through a triangular $\eta^2$ transition state, the windscreen-wiper mode could also include a ring-slippage mechanism via $\eta^1$-$\eta^3$-$\eta^5$ bonding of the tin atom, as observed earlier for nickel,[9] although in this case an inversion of the pyramidal phosphorus atom would be excluded. This assumption follows a general feature of P-chiral phosphanes, which can exist as a pair of stable enantiomers at ambient temperatures.[10,11] A well characterised example of the inversion barrier at a phosphorus[12] or arsenic centre in a five-membered ring exists,[13] and the energy barriers in these cases are anticipated to be much higher than for the triphospholyl system.

If $d^8$- or $d^{10}$-transition metal ions like $Ni^{2+}$,[14] $Pt^{2+}$,[15] $Cu^+$,[16] $Ag^+$,[17] or $Au^+$[18] are bound to a formal 1,2,4-triphospholyl anion, the metal atom may be coordinated by a P-atom lone pair of a planar and aromatic ring ligand. This bonding situation is equivalent to that of a potential inversion transition state for a P substituent that changes sides

[a] Department Chemie und Pharmazie and Interdisciplinary Center for Molecular Materials, Universität Erlangen-Nürnberg, Egerlandstr. 1, 91058 Erlangen, Germany
Fax: +49-9131-852-7367
E-mail: ulrich.zenneck@chemie.uni-erlangen.de
[b] Computer-Chemie-Centrum der Universität and Interdisciplinary Center for Molecular Materials, Nägelsbachstrasse 25, 91054 Erlangen, Germany
Fax: +49-9131-852-6565
E-mail: tim.clark@chemie.uni-erlangen.de
Supporting information for this article is available on the WWW under http://www.eurjic.org or from the author.

  

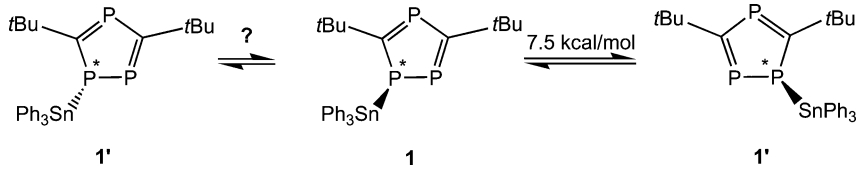


Figure 1. [1,5]-Sigmatropic shift of the $SnPh_3$ group of **1**.

of a phosphole derivative. Phosphole transition metal complexes of $Ti^{4+}$, $Zr^{4+}$ and $Hf^{4+}$ have been shown to exhibit fluxional behaviour using their chiral planarity, and the change of ring face of the substituent was confirmed by facile isomerisation at ambient temperature to form *rac* and *meso* isomers.[19] Even more closely related to other main group element substituents, the bulky $CH(SiMe_3)_2$ group generates planar 1-$CH(SiMe_3)_2$-3,5-di-*t*Bu-1,2,4-triphosphole if attached to one of the neighbouring phosphorus atoms by a covalent P–C bond.[20] The occurrence of planar P atoms has also been attributed to electronic effects.[21]

In this paper we report an experimental and theoretical investigation of the mobility of the stannyl groups of P-chiral 3,5-di-*tert*-butyl-1-(triorganylstannyl)-1,2,4-triphospholes. To allow the observation of a change of face of the tin atom through phosphorus atom inversion by NMR spectroscopy, a chiral Sn substituent is required to transform the two enantiomers of **1** into a pair of diastereomers **2**. The target asymmetrically substituted 1-stannyl-1,2,4-triphospholes are also relevant to an interesting preparative question: a high-yield, highly diastereoselective cycloaddition reaction of **1** with two equivalents of the P-alkyne *t*BuC≡P gives access exclusively to one pair of enantiomeric $P_5(CR)_4(SnR_3)$ cage compounds with seven stereogenic centres.[7] Control of the stereochemistry of such cage-forming processes is one of the main objectives of this research. To the best of our knowledge, no asymmetric P–C cage compounds with a defined stereochemistry are known. We regard such compounds as novel chiral building blocks with several potential uses, for instance as ligands in enantioselective catalysis or in materials science.

## Results and Discussion

Becker et al. have shown that reduction of the stable phosphaalkene $Me_3SiP{=}C(OSiMe_3)(t\text{Bu})$ (**3**) with elemental alkali metals (M) or suitable metal–organic compounds (MR) leads to a mixture of the salts M(2,4,5-tri-*tert*-butyl-1,3-diphospholyl) (M**4**) and M(3,5-di-*tert*-butyl-1,2,4-triphospholyl) (M**5**) as the main products.[22–24] Such mixtures can be separated by repeated fractional crystallisation of the sodium salts from thf. 1-Triorganylstannyl-1,2,4-triphospholes are accessible from the sodium salt Na**5** upon treatment with the corresponding triorganyltin chloride ($R_3SnCl$, **6**).[7]

One chiral group is sufficient to apply this approach to formation of the asymmetrically substituted $Ph_2R^*SnCl$ derivatives **7**. Phenyl groups have been chosen as co-substituents because of their supporting role in forming solid phases of crystallographic quality. The chiral group is preferably introduced with the help of Grignard reagents formed from the corresponding chlorides R*Cl (R* should not contain functional groups to avoid unwanted side reactions). Another problem is the danger of epimerisation of the α-carbon atoms linked to tin. Thus, bornyl and menthyl chlorides and compounds **8c**–**8e**, which contain methylene or *m*-phenylene spacer groups, were used to prevent loss of optical activity (Scheme 1).

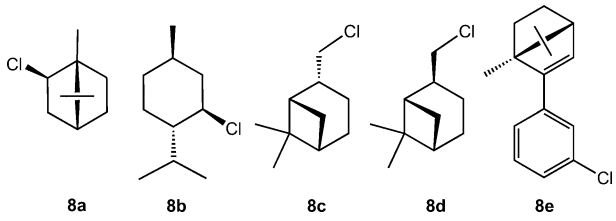


Scheme 1. The chiral organyl chlorides used in this study.

### Chiral Organyl Chlorides R*Cl

Compound **8a** is accessible by addition of HCl to α-pinene at low temperature followed by a Wagner–Meerwein rearrangement.[25] NMR spectroscopy reveals the presence of about 10% of the *endo* isobornyl chloride as an impurity, which could not be removed.[26] (1*R*)-(–)-Menthyl chloride (**8b**) is available commercially. The optically active alcohols (–)-*cis*- and (–)-*trans*-myrtanol were transformed into the corresponding chloro compounds **8c** and **8d** by a standard substitution reaction sequence.[27] To prepare a closely related chiral derivative of 1-(triphenylstannyl)-1,2,4-triphosphole (**1**), which was investigated in most detail, 2-(*m*-chlorophenyl)bornyl-2-ene (**8e**) was synthesised from 1-bromo-3-chlorobenzene and (+)-camphor (Scheme 2).[28]

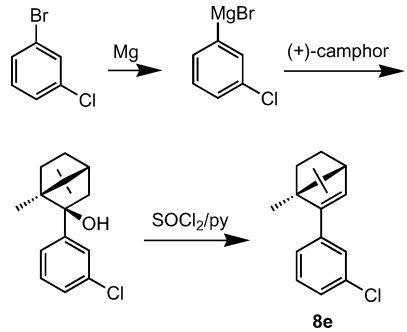


Scheme 2. Preparation of 2-(3-chlorophenyl)bornyl-2-ene (**8e**).

  

### Chirally Modified Triorganyltin Chlorides

The organyl chlorides **8a**–**e** were transformed into the corresponding Grignard compounds by treatment with activated magnesium[29] and then treated with $Ph_2SnCl_2$ to afford the $Ph_2SnR^*Cl$ derivatives **7a**–**e** in yields of about 40% after chromatographic purification to remove unreacted starting material and disubstituted by-product $Ph_2SnR^*_2$ (Scheme 3).[30]

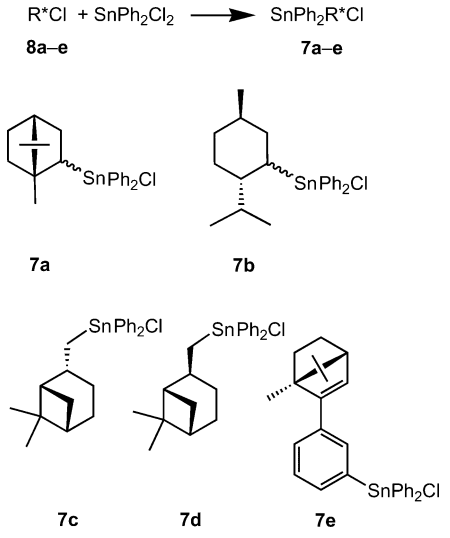


Scheme 3.

In the case of **7a**, only an oily mixture of *exo* and *endo* isomers was obtained.[31] Compound **7b** forms an epimeric mixture of (*R*)-**7b** and (*S*)-**7b**,[32,33] with the main epimer (*R*)-**7b** accounting for about 90% of the mixture. Compounds **7c**–**e** were isolated as chemically and optically pure compounds, and (*R*)-**7b** and **7c** were structurally characterised by X-ray diffraction (Figure 2).

The single-crystal X-ray diffraction studies of (*R*)-**7b** and **7c** reveal that they consist of discrete mononuclear molecules in the solid state. Both these compounds crystallise in chiral space groups ($P2_1$ for **7b** and $P2_12_12_1$ for **7c**) which are composed of a single enantiomer of the corresponding molecules [absolute structure parameter $x = 0.16(10)$ for **7b** and –0.03(1) for **7c**].[34] Compound **7b** contains two independent molecules of one enantiomer in the asymmetric part of the unit cell; two others are symmetry related and the structural differences between the two independent molecules are only marginal (Table 1). The crystal packing of **7b** is characterised by individual stacks of independent molecules along the crystallographic *b* axis that exhibit short Cl···Sn distances of 369 pm between neighbouring molecules. This stacking results in infinite almost linear Cl···Sn–Cl···Sn chains with an Sn···Cl–Sn angle of 170°.

Table 1. Selected Sn–C, C–C and Sn–Cl distances [pm] and angles [°] for triorganyltin chlorides (*R*)-**7b** and **7c**.

| | (*R*)-**7b** (molecule 1) | (*R*)-**7b** (equiv. positions molecule 2) | **7c** |
|---|---|---|---|
| Sn1–Cl | 240.4(5) | 239.6(7) | 239.52(4) |
| Sn1–C1 | 214(1) | 214(2) | 213.4(2) |
| Sn1–C11 | 214(1) | 216(2) | 214.2(2) |
| Sn1–C21 | 213(1) | 213(2) | 212.9(2) |
| C1–C2 | 165(2) | 169(2) | C2–C3 155.4(2) |
| C2–C3 | 139(2) | 133(2) | C3–C4 155.4(3) |
| C3–C4 | 159(2) | 157(2) | C4–C5 152.5(3) |
| C4–C5 | 159(2) | 158(2) | C5–C6 154.4(3) |
| C5–C6 | 146(2) | 142(2) | C6–C7 155.2(2) |
| C6–C1 | 147(2) | 148(2) | C7–C2 153.6(3) |
| C1–Sn1–Cl1 | 100.0(4) | 101.1(6) | 106.10(4) |
| C1–Sn1–C11 | 116.1(5) | 113.4(6) | 112.63(6) |
| C1–Sn1–C21 | 121.4(5) | 125.0(6) | 118.97(7) |
| C11–Sn1–C21 | 111.9(4) | 110.8(5) | 116.20(6) |
| C11–Sn1–Cl1 | 102.0(4) | 101.0(5) | 100.94(5) |
| C21–Sn1–Cl1 | 100.8(5) | 100.8(5) | 98.35(5) |
| C6–C1–C2 | 108(2) | 110(2) | C7–C2–C3 111.3(2) |
| C1–C2–C3 | 117(2) | 121(2) | C2–C3–C4 115.1(2) |
| C2–C3–C4 | 108(2) | 109(2) | C3–C4–C5 112.8(2) |
| C3–C4–C5 | 111(2) | 122(2) | C4–C5–C6 108.2(2) |
| C4–C5–C6 | 106(2) | 107(2) | C5–C6–C7 86.0(2) |
| C5–C6–C1 | 116(2) | 115(2) | C6–C7–C2 107.6(2) |

The single crystal of **7c** investigated contains one independent molecule in the asymmetric part of the unit cell; three more are symmetry related by the three twofold screw axes of the space group. Similar to **7b**, the crystal packing of **7c** is characterised by relatively short intramolecular Cl···Sn distances of 368 pm between neighbouring molecules, which results in the formation of stacks along the crystallo-

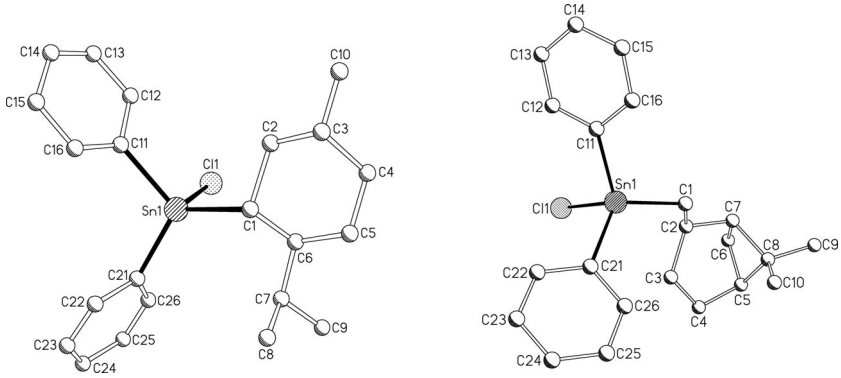


Figure 2. Molecular structures of (1*R*)-(–)-menthyldiphenyltin chloride [(*R*)-**7b**, left] and (–)-*cis*-myrtanyldiphenyltin chloride (**7c**, right) in the solid state.

  

graphic *b* axis. In contrast to (*R*)-**7b**, however, molecules of **7c** are arranged in a zigzag fashion with an Sn···Cl–Sn angle of 124° in the resulting Cl···Sn–Cl···Sn chains. Both these compounds are therefore triorganyltin chlorides with expanded C–Sn–C and reduced C–Sn–Cl angles compared to an ideal tetrahedral arrangement of Sn substituents (Table 1). This effect is more pronounced for (*R*)-**7b** due to direct bonding of the tin atom to the chiral cycle.

As hoped for, the stereochemistry of the chiral organic substituents of (*R*)-**7b** and **7c** remains unchanged in comparison to the starting materials **8b** and **8c**. The C–C bond lengths for the menthyl groups of the two independent molecules of (*R*)-**7b** span the range from 133 to 168 pm and the C–C–C bond angles vary from 106° to 122°. The relative trends within the aliphatic rings are the same for both compounds: the highly $Ph_2SnCl$-influenced C1–C2 bonds and their counterparts in molecule 2, for example, exhibit the significantly elongated distances of 165 and 169 pm, whereas all the other C–C bonds are shorter then 160 pm. Due to a smaller interaction between the stannyl group and the aliphatic *cis*-myrtanyl moiety because of the methylene linker, the intra-ring C–C myrtanyl bond lengths of **7c** fall in the range 152 to 157 pm whereas the C–C–C angles vary from 84° to 115°. All values below 90° belong to internal C–C–C bond angles of the four-membered ring substructure; the others fall in the range 107–115°. In both cases, the molecular structure parameters of the aliphatic chiral groups agree with earlier findings for related compounds,[35] therefore (*R*)-**7b** and **7c** exhibit no unusual strain within the molecules.

### Diastereomeric 1-(Triorganylstannyl)-1,2,4-triphospholes 2a–e

Treatment of the triorganyltin chlorides **7a**–**e** with 3,5-di-*tert*-butyl-1,2,4-triphospholylsodium (Na**5**) in toluene at –30 °C led to formation of the target diastereomeric 1-(triorganylstannyl)-3,5-di-*tert*-butyl-1,2,4-triphospholes **2a**–**e** in yields of up to 80%. Compounds **2a**,**b**,**d** were isolated as yellow crystals that proved to be suitable for X-ray diffraction studies, whereas **2e** was isolated as an amorphous solid and **2c** as a yellow oil.

As indicated by the properties of the isomeric bornyl chloride **7a**, a double set of signals with an intensity ratio of about 2:1 in the NMR spectra of bornyl derivative **2a** proves the loss of at least one stereogenic centre. As no optical activity at all remained from the starting α-pinene, a complete racemisation of the norbornyl group is assumed to form a mixture of bornyl and isobornyl derivatives[25] (see below). Both these compounds exist as diastereomers in rapid equilibrium with the two enantiomeric stannyl-1,2,4-triphosphole units. A double set of NMR signals in the same 9:1 ratio as for the (*R*)-**7b**/(*S*)-**7b** starting material in the menthyl derivative **2b** suggests that no further epimerisation of the menthyl group takes place upon connecting the tin atom to the heterocycle. The spectroscopic investigations gave no indication of epimerisation or racemisation of compounds **2c**,**d**,**e** (Scheme 4), all of which show only one set of $^1H$, $^{13}C$ and $^{31}P$ NMR signals and are optically active.

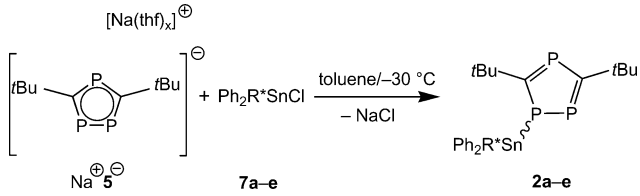


Scheme 4. Preparation of diastereomeric 3,5-di-*tert*-butyl-1-(triorganylstannyl)-1,2,4-triphospholes **2a**–**e**.

The molecular structures of **2a**,**b**,**d** in the solid state are shown in Figures 3, 4 and 5, respectively, and selected bond angles and lengths are given in Table 2. Compounds **2a**,**b**,**d** exhibit some general structural features that are similar to the $Ph_3Sn$ derivative **1**,[7] such as the pyramidality of the $\lambda^3$-phosphorus atoms, which is characterised by the sum of the bond angles around P1 [Σ∢P1]. The two enantiomers of **1** have values of 310.3°, whereas all enantiomers and epimers of **2a**,**b**,**d** characterised structurally in this study exhibit values of between 292.9° and 312.6° (Table 2). Consistent with this observation, the triphosphole moieties form almost planar P=C–P=C trapezoids with alternating P–C bond lengths. The $\lambda^3$-P centre is only slightly displaced from this plane opposite to the side of the tin atom to form envelope-type conformers of the five-membered rings. These findings give a clear indication of localised $\pi^4$-systems and a pyramidal phosphorus atom as a linker which is not involved in π-interactions with the neighbouring $sp^2$-hybridized ring carbon and phosphorus atoms. A significant influence of the chiral tin substituents on the bonding situation of the triphosphole ring can be ruled out.

The specific structural features of the molecules in the solid state are as follows. The *exo*-bornyl derivative **2a** crystallises in the centrosymmetric space group $P\bar{1}$. The two molecules in the unit cell form a racemic mixture of two enantiomers that are crystallographically connected by an inversion centre (Figure 3). One and a half molecules of tol-

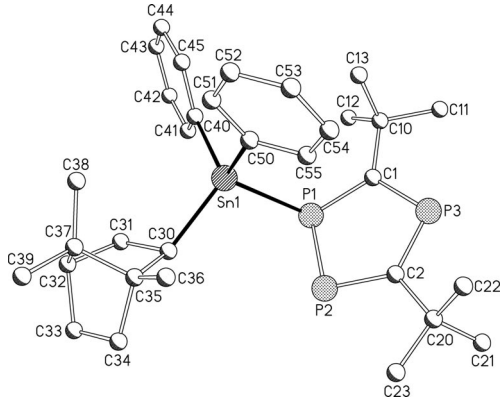


Figure 3. Molecular structure of one of the enantiomers of racemic *exo*-derivative **2a** in the solid state. Solvent molecules and hydrogen atoms have been omitted for clarity.

  

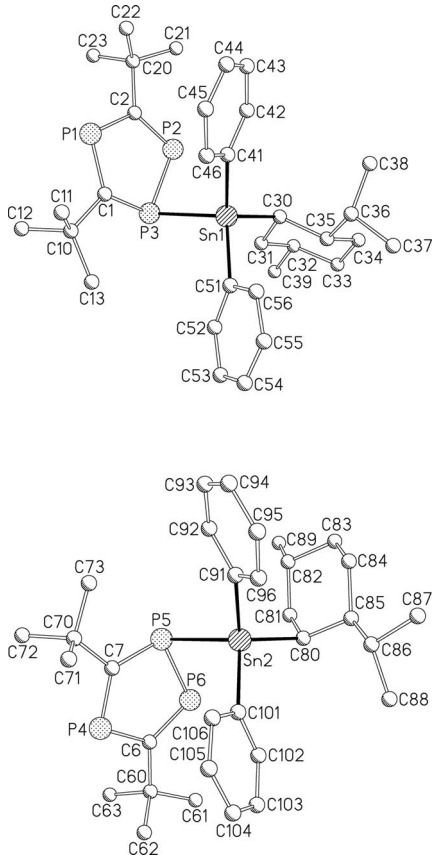


Figure 4. Molecular structures of two epimers of **2b** (*SR*; top, equatorial) and **2b** (*RS*; bottom, axial) in the solid state. Hydrogen atoms have been omitted for clarity.

uene are also present per formula unit. The single toluene molecule occupies a specific position in the unit cell whereas the half molecule is disordered around the crystallographic inversion centre. No hydrogen atom positions associated with this molecule were determined. The inversion relation between the two observed enantiomers of **2a** proves a complete racemisation of the bornyl group with its three stereogenic centres at C30, C32, and C35 and the presence of both (*R*)- and (*S*)-P1. Molecules of **2a** form stacks along the crystallographic *c*-direction, and four of these stacks at the unit cell edges form a channel that is occupied by the toluene solvent molecules. All bond lengths and angles of the aliphatic *exo*-bornyl substituent are in the normal range of values for derivatives, with no significant distortion.[36]

Crystals of **2b** of sufficient quality for X-ray diffraction studies were only obtained for a crystalline phase composed of a 1:1 mixture of the two epimers already observed for stannyl chloride **7b**. The main epimer can only be isolated as an amorphous solid and attempts to separate the solid phases of **2b** by fractional crystallisation failed. Compound **2b** crystallises in the chiral space group *P*1 [absolute structure parameter $x = 0.015(16)$][34] with two independent molecules in the unit cell that represent two diastereomers with opposite stereodescriptors for P3 (*S*) and P5 (*R*) and C30 (*R*) and C80 (*S*), the menthyl group stereogenic centre that is partially lost by the tin-α-$C_{menthyl}$ interaction (Figure 4). The other two stereogenic centres of the menthyl group (C32–C35 and C82–C85) remain unaffected by all chemical procedures that eventually lead to **2b**. The two phenyl tin substituents of two neighbouring independent epimers are involved in weak T-shaped π-stacking interactions in the crystalline phase. The corresponding C(H)··· π distances are 362 and 368 pm.

As intended, the introduction of achiral spacer groups like methylene or *m*-phenylene between the tin atom and the next stereogenic centre prevents epimerisation or racemisation of the chiral organyl group of compounds **2c**,**d**,**e** completely. The structure of *trans*-myrtanyl species **2d** was determined by X-ray diffraction (Figure 5). This compound crystallises in the chiral space group $P2_1$ with two independent molecules in the asymmetric part of the unit cell. These two molecules are diastereomers with the tin atom bound to either of the two adjacent diastereotopic (*R*)- and (*S*)-phosphorus centres but with identical stereochemistry [the same as that of the starting material (–)-*trans*-myrtanol] of the chiral auxiliary group [absolute structure parameter $x = 0.009(11)$].[34] These two epimeric molecular structures represent the start and end points of the [1,5]-sigmatropic stannyl shift in **2b**. As the closest stereogenic centres are separated by three bonds, epimerisation of the $\lambda^3$-phospho-

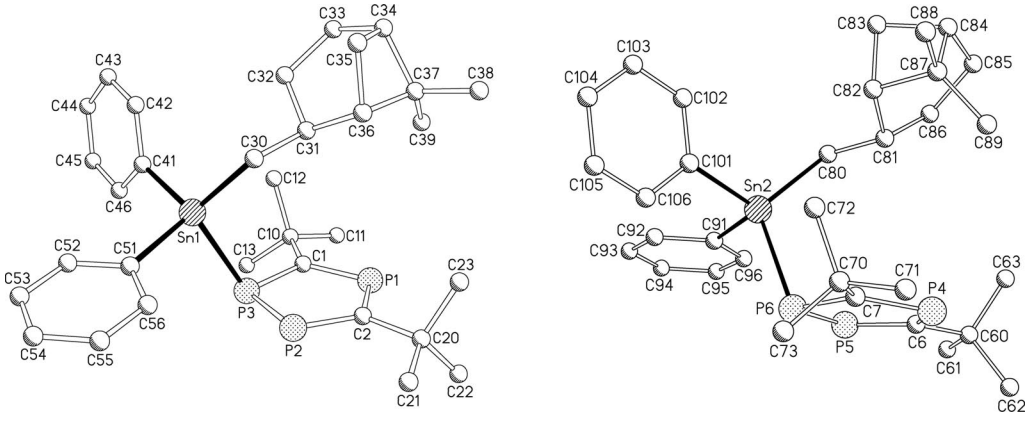


Figure 5. Molecular structure of the two diastereomers **2d** (*SS*, left) and **2d** (*RS*, right) in the solid state. Hydrogen atoms have been omitted for clarity.

  

Table 2. Selected bond lengths [pm] and angles [°] for racemic **2a**, epimeric **2b** (*SR*)/(*RS*), diastereomeric **2d** (*SS*)/(*RS*), and calculated values of the energetic minimum species **9a** ($R^1 = R^2 = R^* = Me$).[a]

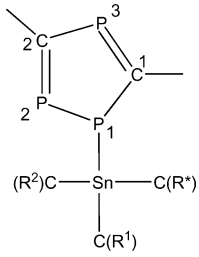


| | **2a** | **2b**(*SR*) | **2b**(*RS*) | **2d**(*SS*) | **2d**(*RS*) | **9a** |
|---|---|---|---|---|---|---|
| Sn–P1 | 254.95(9) | 255.9(2) | 257.3(12) | 255.1(1) | 254.84(9) | 259.0 |
| Sn–C(R*) | 217.0(3) | 217.3(6) | 220.5(6) | 215.2(3) | 216.1(3) | 214.3 |
| Sn–C($R^1$) | 214.1(3) | 212.7(6) | 216.3(7) | 215.1(3) | 215.6(3) | 214.7 |
| Sn–C($R^2$) | 214.7(3) | 214.3(7) | 216.7(6) | 214.8(4) | 214.5(3) | 214.9 |
| P1–C1 | 177.3(3) | 178.7(6) | 176.9(7) | 178.5(4) | 178.9(4) | 179.5 |
| C1–P3 | 171.7(3) | 173.1(7) | 169.0(7) | 170.9(4) | 171.9(4) | 173.2 |
| P3–C2 | 176.5(4) | 175.9(7) | 178.3(7) | 178.5(4) | 177.6(4) | 179.3 |
| C2–P2 | 171.9(3) | 171.0(6) | 170.3(7) | 171.0(4) | 171.7(4) | 173.4 |
| P2–P1 | 213.2(2) | 215.1(2) | 214.3(3) | 213.8(2) | 214.5(2) | 219.9 |
| C($R^2$)–Sn–C(R*) | 119.6(2) | 116.5(2) | 110.7(2) | 110.7(2) | 116.0(2) | 112.6, 111.3, 111.3 |
| C($R^2$)–Sn–P1 | 107.87(9) | 108.5(2) | 106.0(2) | 101.43(9) | 108.08(9) | 106.5 |
| C($R^1$)–Sn–P1 | 105.4(1) | 107.4(2) | 107.3(2) | 109.8(1) | 103.75(8) | 110.0 |
| C(R*)–Sn–P1 | 101.94(9) | 106.0(2) | 109.2(2) | 110.6(1) | 115.6(1) | 104.8 |
| C1–P1–Sn | 114.8(2) | 104.8(2) | 107.0(3) | 114.0(2) | 112.0(1) | 101.6 |
| P2–P1–Sn | 96.21(4) | 87.02(8) | 88.04(8) | 93.79(4) | 88.97(4) | 98.2 |
| C1–P1–P2 | 101.6(2) | 101.1(2) | 99.0(2) | 100.8(2) | 100.7(2) | 98.9 |
| P3–C1–P1 | 116.6(2) | 116.1(4) | 119.8(4) | 117.5(2) | 117.4(2) | 121.5 |
| C1–P3–C2 | 102.1(2) | 103.2(3) | 101.6(3) | 101.9(2) | 102.1(2) | 97.8 |
| P2–C2–P3 | 121.6(2) | 121.2(4) | 120.2(4) | 121.2(2) | 121.3(2) | 125.4 |
| C2–P2–P1 | 97.1(2) | 98.0(2) | 99.0(2) | 97.9(2) | 97.9(2) | 95.7 |
| Σ∢P1 | 312.6 | 292.9 | 294.0 | 308.6 | 301.7 | 298.7 |

[a] Experimental data: C($R^1$) = C($R^2$) = $C_{ipso}$ of phenyl groups; C(R*) = C of chiral group next to the tin atom. General notation **2x**(*AB*): *A* = configuration of $\lambda^3$-phosphorus atom that carries the stannyl group, *B* = configuration of the stereogenic centre next to the tin atom of the chiral auxiliary group.

rus atom does not influence the structural parameters of the myrtanyl group significantly − only the relative orientation of these two building blocks of **2b** changes, mainly by rotation around the C–C bonds C30–C31 and C80–C81. This may be caused by packing effects. Both phenyl substituents of both diastereomers are involved in weak T-shaped π-stacking interactions in the solid state with C(H)···π-distances ranging from 355 to 409 pm.

### NMR Spectra and Fluxional Behaviour of Diastereomeric Stannyltriphospholes

The general appearance of the NMR spectra of **2c**,**d**,**e** at ambient temperature is very similar to that of the achiral version **1**[7] except that the chiral groups contribute to the spectra. Unlike **2a**,**b**, all three exhibit one set of signals in their $^1H$, $^{13}C$ and $^{31}P$ NMR spectra, which is consistent with the optical purity of the compounds and a highly mobile tin atom with respect to the triphospholyl moiety. The solution $^1H$ NMR spectra, for example, always show only one sharp resonance for the *t*Bu groups of the heterocycle even though they are not equivalent in the solid state. The same situation occurs for the $^{31}P$ NMR spectra, which are characterised by $AB_2X$ spin systems (X = $^{117/119}Sn$) at ambient temperature with triplets for the A nucleus at around $\delta$ = 325 ppm and doublets close to $\delta$ = 160 ppm for the two B nuclei ($^2J_{P,P} \approx 40$ Hz) (Figure 6). Both are accompanied by $^{117/119}Sn$ satellites with a smaller coupling to the A-nucleus ($^3J_{Sn,P} \approx 50$ Hz) and higher values for B ($^1J_{Sn,P} \approx 350$ Hz). The variable-temperature $^{31}P\{^1H\}$ NMR spectra of the two spectroscopically distinguishable diastereomers of **2a**, for example, reveal some details. Thus, the A-parts of both spectra remain almost unchanged on cooling to –70 °C, with only some line broadening due to increasing solvent viscosity leading to a loss of the triplet appearance of the lines at the low-temperature limit of the experiment (–85 °C). In contrast, the B-parts of the spectra lose their tin satellites at –10 °C due to line broadening caused by slowing down of the [1,5]-sigmatropic shift, their doublet appearance is no longer visible at –30 °C, and at –70 °C they are no longer observable at all. These signals do not reappear at temperatures down to –85 °C, therefore no slow-exchange-limit spectra could be obtained and a direct determination of the coalescence temperature, and thus the energy barrier, was not possible. As the $^{31}P$ NMR spectra of solutions of **1** behave similarly on cooling, the activation

  

energy of all derivatives of **2** investigated is estimated to be close to the value ($\Delta G^{\ddagger} \approx 7.5$ kcal mol$^{-1}$) found for this compound.[7]

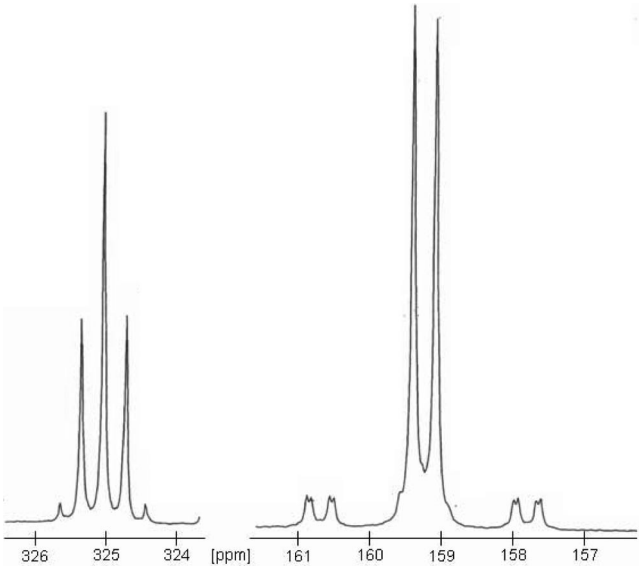


Figure 6. $^{31}P\{^{1}H\}$ NMR spectrum (121.49 MHz, $CDCl_3$, 25.1 °C) of 1-{[3-(2-bornyl-2-ene)phenyl]diphenyltin}-3,5-di-*tert*-butyl-1,2,4-triphosphole (**2e**).

Replacement of the achiral $Ph_3Sn$ group in **1** by $SnPh_2R^*$ would be expected to give an ABCX spin-system if the tin atom were to oscillate only between the two adjacent phosphorus atoms in the suprafacial windscreen-wiper mode between the two diastereomeric minima **A** and **B** (Scheme 5). Exchange of the stereochemical identity of the phosphorus atoms starting from state **A** to form identical **A′** is possible either via state **B** and planar transition state $\mathbf{T_i}'$, if the process begins with the 1,5-shift, or via $\mathbf{T_i}$ and **B′**, if the inversion of the pyramidal phosphorus atom is the initial step. The molecules must pass through the planar inversion transition states $\mathbf{T_i}$ or $\mathbf{T_i}'$ to generate the observed $AB_2X$ spin

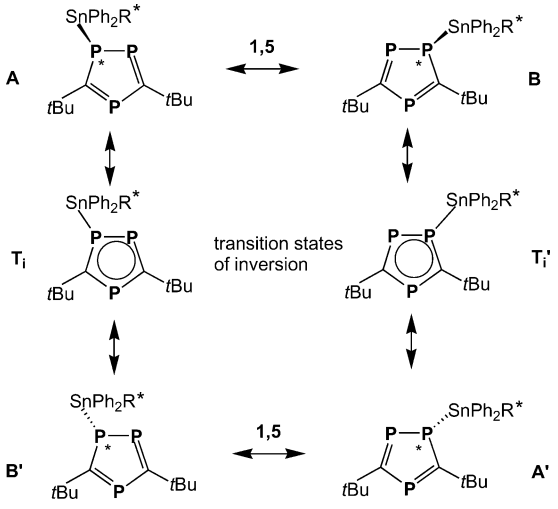


Scheme 5. Diastereomeric ground states (**A** and **B**) at equilibrium and inversion transition states ($\mathbf{T_i}$) of 1-(triorganylstannyl)-1,2,4-triphosphole derivatives **2**.

system in both cases. A projection of the cyclic rocking mode of the stannyl group in front of the $P_2$-edge of diastereomeric 1,2,4-triphospholes **2**, as deduced from the dynamic NMR spectra, is shown in Figure 7.

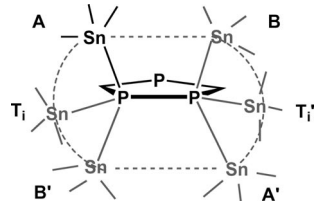


Figure 7. Cyclic rocking mode of the mobile stannyl group in front of the $P_2$-edge of 1-(triorganylstannyl)-1,2,4-triphospholes **2**.

## Computational Results

Density functional theory (DFT) calculations were performed on the model compound trimethylstannyl-1,2,4-triphosphole (**9**) in order to analyse the bonding situation of compounds **1** and **2** and the principal aspects of the mobility of the stannyl group in the vicinity of the 1,2,4-triphosphole ring. The absence of bulky carbon substituents in the model compound means that the DFT studies emphasise the electronic aspects of the molecular dynamics.

All calculations were performed with the Gaussian03 suite of programs[37] and the LANL2DZ basis set with standard pseudopotentials[38] and an additional set of polarisation functions[39] (designated LANL2DZ+pol in the following). Optimisations and calculations of the normal vibrations were carried out using density-functional theory with the Becke three-parameter/Lee–Yang–Parr hybrid functional.[40] Single-point calculations were performed on the B3LYP/LANL2DZ+pol optimised geometries using the same basis set but with an additional set of polarisation functions on hydrogen[39] (designated LANL2DZ+2pol in the following) and at the coupled cluster level including single and double excitations[41] and a non-iterative correction for triples[42] [CCSD(T)]. Minima and transition states were confirmed as such by calculating their normal vibrations within the harmonic approximation at the B3LYP/LANL2DZ+pol level. The energies discussed in the text are those calculated at the CCSD(T)/LANL2DZ+2pol level corrected for zero-point vibrational energy using the unscaled zero-point energies calculated at the B3LYP/LANL2DZ+pol level.

All principal isomers of **9** with an 1,2,4-triphosphole skeleton and a $Me_3Sn$ group with Sn–P and Sn–$C_{ring}$ bonds were considered. Three minima − **9a**, **9b**, and **9c** − were identified for **9** in close energetic proximity. The global minimum **9a** represents the P-chiral 1-stannyl-1,2,4-triphosphole case, which has been observed experimentally for all stannyl-1,2,4-triphospholes in solution and in the solid state reported so far (Table 3 and Figure 8).

The transition states (structures with one imaginary frequency) are designated $\mathbf{T_s(9n{\rightarrow}m)}$ for suprafacial $SnMe_3$-shift transition states between structures **9n** and **9m** and as

  

Table 3. Calculated total, zero-point vibrational and relative energies of the isomers of model compound **9**.

| Species | B3LYP/LANL2DZ+pol | | | | CCSD(T)/LANL2DZ+2pol | |
|---|---|---|---|---|---|---|
| | Total energy[a] | $N_{imag}$[b] | ZPE[c] | $E$(rel)[d] | Total energy[a] | $E$(rel)[d] |
| **9a** | –220.09207 | 0 | 90.49 | 0.0 | –219.32744 | 0.0 |
| **9b** | –220.08832 | 0 | 90.44 | 2.3 | –219.32249 | 3.1 |
| **9c** | –220.08630 | 0 | 90.62 | 3.8 | –219.32581 | 1.2 |
| $\mathbf{T_s}$**(9a→a′)** | –220.08260 | 1 | 90.45 | 5.9 | –219.31880 | 5.4 |
| $\mathbf{T_s}$**(9a→b)** | –220.07925 | 1 | 90.57 | 8.1 | –219.31841 | 5.7 |
| $\mathbf{T_s}$**(9b→c)** | –220.07775 | 1 | 90.61 | 9.1 | –219.31632 | 7.1 |
| $\mathbf{T_s}$**(9a→c)** | –220.08222 | 1 | 90.67 | 6.4 | –219.32054 | 4.5 |
| $\mathbf{T_s}$**(9b→b′)** | transition state not located | | | | | |
| $\mathbf{T_i}$**(9a)** | –220.08580 | 1 | 90.53 | 4.0 | –219.31906 | 5.3 |
| $\mathbf{T_i}$**(9c)** | –220.08137 | 1 | 90.38 | 6.6 | –219.31309 | 8.9 |

[a] Total energy in hartrees. [b] Number of imaginary frequencies at the B3LYP/LANL2DZ+pol level. [c] Zero-point vibrational energy (kcal mol$^{-1}$) at the B3LYP/LANL2DZ+pol level. [d] Calculated energy (including an unscaled B3LYP/LANL2DZ+pol ZPE correction) relative to **9a** (kcal mol$^{-1}$).

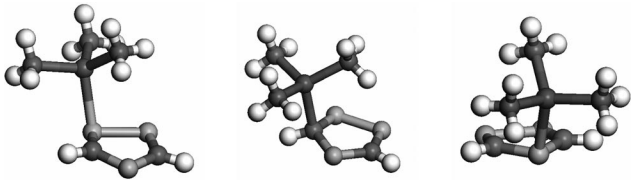

Figure 8. Calculated structures of (trimethylstannyl)-1,2,4-triphosphole isomers **9a** (left), **9b** (middle) and **9c** (right). The CCSD(T)/LANL2DZ+2pol relative energies [kcal mol$^{-1}$] of the three minima are **9a**: 0.0, **9b**: 3.1, and **9c**: 1.2.

$\mathbf{T_i}$**(9n)** for inversion transition states for the $\lambda^3$-phosphorus atom. The data shown in Table 3 are summarised schematically in Figure 9.

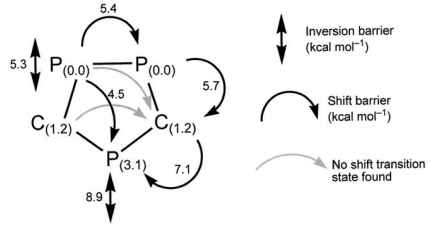


Figure 9. Shift-barrier calculation results [kcal mol$^{-1}$] for **9**.

With the exception of the simplified substituents, the calculated structural parameters of **9a** (Table 2) are all close to the X-ray data reported for the 1-stannyl-1,2,4-triphospholes **2** in the solid state in this paper and those of **1**,[7] thus suggesting that **9** is an adequate model and that the level of calculation is appropriate.

All meaningful reaction pathways for migration of the stannyl group between the minima **9a**, **9b** and **9c** were calculated. The resulting energy barriers are summarised in Figure 9.

The calculations confirm the experimental results. There is considerable variation between the B3LYP and CCSD(T) results, however, which means that no firm conclusions can be drawn about the relative ease of the multitude of competing rearrangements or even the relative stability of the three competing isomers. However, **9a** is found to be the most stable structure at both levels and both **9b** and **9c** are calculated to lie within 4 kcal mol$^{-1}$. The 1,2-P→P shift (**9a→9a′**) has an activation energy of 5–6 kcal mol$^{-1}$. The 1,5-P→C shift (**9a→9b**) and 3,4-C→P shift (**9b→9c**) are calculated to have less stable transition states, but the 1,4-P→P shift (**9a→9c**) is similar in energy to the 1,2-P→P shift. Direct inversion at P1 of **9a** is easier than that at P4 of **9c** and is close in energy to the easiest $SnMe_3$ shifts.

The most apparent feature of Figure 9 is the small range of values for the energy barriers, which span a factor of only two and include the estimated experimental value of 7.5 kcal mol$^{-1}$. In agreement with the NMR spectroscopic findings, the energy required for inversion at P1 or for the suprafacial 1,2-shift, which both represent epimerisation of P-chiral **9a**, are calculated to be almost identical. A 30% smaller calculated absolute value may be attributed to the simplifications of model compound **9**, which lacks the bulky *t*Bu carbon substituents of the derivatives of **2**. The energetic minima **9b** and **9c**, the transition state for the inversion of P4 $\mathbf{T_i}$**(9c)** and the suprafacial shift processes, with the exception of P1–P2, can be expected to be destabilised to some extent with respect to **9** by the bulky *tert*-butyl groups for the compounds investigated experimentally. The calculated inversion transition states $\mathbf{T_i}$ (Figure 10) and suprafacial $SnMe_3$ group shift $\mathbf{T_s}$ (Figure 11) illustrate this point.

Figure 10. Calculated ring inversion transition states $\mathbf{T_i}$ for **9a** (left) and **9c** (right).

The transition states expected to be influenced least by C substituents are $\mathbf{T_i}$**(9a)** and that for the suprafacial stannyl group shift $\mathbf{T_s}$**(9a→a′)**. Both of these are identical with those postulated on the basis of the NMR spectroscopic properties. Even in the absence of bulky $C_{ring}$ substituents, the highest activation barrier found by the calculations connects 4-stannyl-1,2,4-triphosphole minimum **9c** and its hori-

  

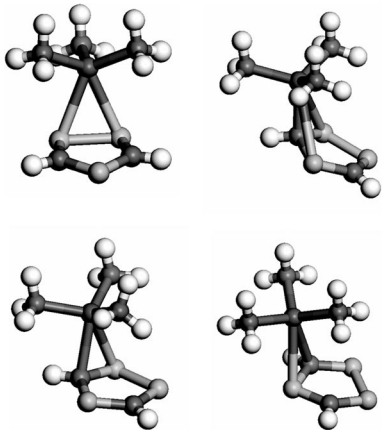

Figure 11. Calculated transition states $\mathbf{T_s}$ of suprafacial P–P (top) and P–C (bottom) stannyl group shifts for **9**.

zontal mirror image **9c′** through inversion transition state $\mathbf{T_i}$(**9c**). As this is a competitive process with higher activation energy it is not observable by dynamic NMR spectroscopy, but **9c** may nevertheless contribute to the mobility of the stannyl groups as a minor component. Variable-temperature NMR spectroscopy of a binuclear W/Cu 1,2,4-triphosphole complex, for example, has shown that the suprafacial exchange of the $Cu^I$ nucleus from P1 or P2 to P4 has an activation barrier of 10.5 kcal mol$^{-1}$.[16]

## Conclusions

Three different diastereomeric 1-triorganyl-1,2,4-triphospholes **2c**,**d**,**e** with optically pure stannyl substituents have been prepared and characterised. Dynamic NMR spectroscopy of the compounds has shown, for the first time, a facile stannyl group shift between the two adjacent P atoms of the heterocycle (P1 and P2) that includes ring inversion with a planar transition state $\mathbf{T_i}$. Nicely in line with the NMR spectroscopic results on diastereomeric derivatives **2c**,**d**,**e**, DFT and ab initio calculations with the simplified model compound (trimethylstannyl)-1,2,4-triphosphole (**9**) have shown that 1-(trimethylstannyl)-1,2,4-triphosphole (**9a**) is the global energetic minimum for **9** and that it undergoes an almost isoenergetic 1,2-shift and ring inversion as the main epimerisation processes of the two enantiomers of **9a**.

## Experimental Section

All reactions were carried out in flame-dried glassware under an oxygen-free atmosphere of dry nitrogen using Schlenk techniques. Solvents were dried by standard methods and distilled under $N_2$. All NMR solvents were carefully dried, degassed and stored over 4-Å molecular sieves. NMR spectra were recorded with JEOL JNM-EX 270, JNM-LA 400 and Bruker Avance DRX 300 spectrometers. $^1$H and $^{13}$C NMR chemical shifts are given relative to residual solvent peaks. $^{31}$P NMR chemical shifts are referenced to external $H_3PO_4$ (85%). Mass spectra were recorded with Varian Mat 212 and JEOL JMS 700 spectrometers. Elemental analysis was performed locally by the microanalytical laboratory at the Department für Chemie und Pharmazie of the University of Erlangen-Nürnberg.

The starting material (3,5-di-*tert*-butyl-1,2,4-triphospholyl)sodium (Na**5**) was prepared by a published route.[7] Diphenyltin dichloride, (+)-camphor, (–)-*cis*/*trans*-myrtanol, 1-bromo-3-chlorobenzene and solvents were purchased from standard commercial sources. Diphenyltin dichloride was recrystallised from dry *n*-hexane. (1*R*,2*R*)-Bornyl chloride (**8a**) was prepared according to a published procedure.[25] The product contains about 10% of the *endo* isomer isobornyl chloride.[26] (1*R*)-(–)-Menthyl chloride (**8b**) was purchased from Fluka and used without further purification. (–)-*cis*- and (–)-*trans*-Myrtanyl chloride **8c/d** were prepared from commercially available (1*S*,2*R*,5*S*)-(–)-*cis*- and (1*R*,2*R*,5*S*)-(–)-*trans*-myrtanol, respectively, as described in the literature.[27] Activated magnesium was generated by reduction of water-free $MgCl_2$ with potassium in thf.[29]

**2-(3-Chlorophenyl)-(1*R*,4*R*)-1,7,7-trimethylbicyclo[2.2.1]hept-2-ene [2-(3-Chlorophenyl)bornyl-2-ene, 8e]:** For preparation of the precursor 2-*endo*-(3-chlorophenyl)borneol, a solution of 1-bromo-3-chlorobenzene (16.77 g, 10.3 mL, 87.6 mmol) in 30 mL of dry thf was added dropwise over 30 min to 50 mL of dry thf containing magnesium turnings (2.13 g, 87.6 mmol). The mixture was heated for an additional two hours at reflux or until the magnesium had dissolved. After this time a solution of (+)-camphor (13.34 g, 87.6 mmol) in dry thf (40 mL) was added and the mixture was heated for an additional 14 h. The reaction mixture was then cooled to approximately 0 °C and was hydrolysed carefully with saturated $NH_4Cl$ solution (ca. 50 mL). Diethyl ether (50 mL) was added to form a biphasic system and the layers separated. The aqueous layer was washed twice more with diethyl ether (20 mL), then the combined organic phases were washed with saturated $NaHCO_3$ solution and water and dried with $Na_2SO_4$. After filtering off the drying agent, the solution was evaporated and excess camphor sublimed ($10^{-2}$ mbar/40–45 °C). Recrystallisation of the solid residue from petroleum ether or *n*-hexane yielded the desired product as colourless thin needles or a powder (10.2 g, 38.6 mmol, 44.1%). $^1$H NMR (399.65 MHz, $CDCl_3$, 27.2 °C): $\delta$ = 0.74 (m, 1 H), 0.84 (s, 3 H, $CH_3$), 0.88 (s, 3 H, $CH_3$), 1.22 (m, 1 H), 1.26 (s, 3 H, $CH_3$), 1.46 (s, 1 H, OH), 1.67 (m, 1 H), 1.72 (s, 1 H), 1.85 (m, 1 H), 2.11 (m, 1 H), 2.19 (d, $^3J_{^1H,^1H}$ = 10 Hz, 1 H), 7.14 (m, 1 H), 7.18 (m, 1 H), 7.32 (m, 1 H), 7.45 (m, 1 H) ppm. $^{13}$C{$^1$H} NMR (100.40 MHz, $CDCl_3$, 27.2 °C): $\delta$ = 10.0 ($CH_3$), 21.89 ($CH_3$), 21.92 ($CH_3$), 26.8, 31.5, 45.9, 46.0, 50.8, 53.9, 83.7 (COH), 125.3, 127.2, 127.5, 129.0, 134.0, 148.5 ppm. MS (FD): *m*/*z* (%) 264 (100) $[M]^+$. $C_{16}H_{21}ClO$ (264.79): calcd. C 72.57, H 7.99; found C 72.85, H 8.19. Optical rotation (23 °C, *c* = 0.0824 in thf): $[a]_{546}$ = –41; $[a]_{578}$ = –36; $[a]_{589}$ = –34; $[a]_{633}$ = –30.

A solution of 2-*endo*-(3-chlorophenyl)borneol (5.0 g, 19 mmol) in pyridine (40 mL) was cooled to –40 °C and thionyl chloride (1.80 mL, 24.8 mmol) was added dropwise. After an additional 30 min of stirring at –40 °C, the cooling bath was removed and the reaction mixture warmed to room temperature. After addition of *n*-hexane (100 mL) the solid was filtered off and the solvent evaporated. Distillation of the residue at $10^{-2}$ mbar and 68–71 °C gave the desired product **8e** as a colourless oil in a yield of 83% (3.9 g, 15.8 mmol). $^1$H NMR ($CDCl_3$, 269.7 MHz, 19.5 °C): $\delta$ = 0.75 (s, 3 H, $CH_3$), 0.80 (s, 3 H, $CH_3$), 1.02 (s, 3 H, $CH_3$), 1.05 (m, 1 H), 1.21 (m, 1 H), 1.60 (m, 1 H), 1.86 (m, 1 H), 2.31 (m, $^3J_{H3,H4}$ = 3.5 Hz, 1 H(4)], 5.95 (d, $^3J_{H3,H4}$ = 3.5 Hz, 1 H(3)], 7.11 (m, 4 $H_{ar}$) ppm. MS (FD): *m*/*z* (%) 246 (100) $[M]^+$.

  

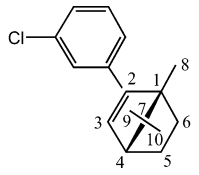


**Preparation of the Chiral Modified Tin Compounds 7a–e. General Procedure:** One mol of the chiral organic chloro compound was added with a syringe directly to a stirred suspension of two mol of activated magnesium in absolute thf and the mixture heated under reflux for an additional three hours. After the reaction mixture had cooled to room temperature it was filtered directly into a rapidly stirring solution of one mol of diphenyltin dichloride in thf. After the addition of a small amount of 4-*tert*-butylcatechol the mixture was stirred overnight. The solvent was evaporated until a white precipitate appeared, then an equal volume of *n*-hexane was added and the suspension was stirred for an additional hour. After filtration the solvent was evaporated and the residue was eluted on silica gel ($SiO_2$/5%$H_2O$) with *n*-hexane/diethyl ether (4:1) as eluent. The desired products were found in the second fraction and were identified by the formation of streaks in the solvent. The triorganyltin chlorides were obtained as colourless oils after evaporation of the solvent. Compounds **7b** and **7c** were crystallised from *n*-hexane at 4 °C as colourless needles.

**{(1*R*,2*R*,4*R*)-1,7,7-Trimethylbicyclo[2.2.1]hept-2-yl}diphenyltin Chloride [(2-Bornyl)diphenyltin Chloride, 7a]:** Obtained as a mixture of *exo* and *endo* isomers. Yield 3.65 g (8.2 mmol, 30.5%). $^1$H NMR (300.13 MHz, $CD_2Cl_2$, 26.9 °C): $\delta$ = 7.48 (m, 10 H, $H_{ar}$), 2.70–0.92 [m, 8H (CH, $CH_2$)], 0.84 (s, 3 H, $CH_3$), 0.80 (s, 3 H, $CH_3$), 0.74 (s, 3 H, $CH_3$) ppm. MS (FD): *m*/*z* (%) 445 (100) $[M]^+$, 308 (2) $[SnCl(C_6H_5)_2]^+$, 137 (10) $[C_{10}H_{17}]^+$.

**2-[(1*S*,2*R*,4*R*)-1-Isopropyl-4-methylcyclohexyl]diphenyltin Chloride [(–)-Menthyldiphenyltin Chloride, 7b]:** Obtained as a 2:1 mixture of (*R*)-**7b** and (*S*)-**7b** epimers before workup (9:1 after repeated recrystallisation). Yield 12.91 g (28.8 mmol, 53.3%).[33] $^1$H NMR spectroscopic data identical with those reported in the literature within the margins of experimental error. $^{13}C\{^1H\}$ NMR (75.47 MHz, $CDCl_3$, 25.0 °C): (*R*)-**7b**: $\delta$ = 141.8/141.5 (s, $C_i$/$C_{i'}$), 135.9 (s, d, $^2J_{117/119Sn,13C}$ = 45.0 Hz, $C_o$), 129.9 (s, d, $^3J_{117/119Sn,13C}$ = 12.9 Hz, $C_p$), 128.9 (s, d, $^4J_{117/119Sn,13C}$ = 55.4 Hz, $C_m$), 46.28 (s, $J_{117/119Sn,13C}$ = 16.5 Hz, $CH_{al}$), 42.01 (s, $CH_{al}$), 39.95 (s, d, $J_{117/119Sn,13C}$ = 27.4 Hz, $CH_2$), 35.58 (s, d, $J_{117/119Sn,13C}$ = 27.4 Hz, $CH_{al}$), 35.32 (s, d, $J_{117/119Sn,13C}$ = 84.7 Hz, $CH_{al}$), 34.93 (s, d, $J_{117/119Sn,13C}$ = 9.9 Hz, $CH_{2/al}$), 26.70 (s, d, $J_{117/119Sn,13C}$ = 89.5 Hz, $CH_{2/al}$), 22.35 (s, 3 H, $CH_3$), 21.79 (s, 3 H, $CH_3$), 15.75 (s, 3 H, $CH_3$); (*S*)-**7b**: $\delta$ = 49.03, 45.56, 38.86, 34.13, 33.98, 33.72, 30.47, 22.27, 21.87, 21.01 ppm. MS (FD): *m*/*z* (%) 447 (100) $[M]^+$, 139 (6) $[(C_{10}H_{19})]^+$, 860 (20) $[M_2 - Cl]^+$. $C_{22}H_{29}ClSn$ (447.63): calcd. C 59.03, H 6.53; found C 59.32, H 6.61. Optical rotation (22 °C, *c* = 0.01 in *n*-hexane): $[\alpha]_{589}$ = –18.0; $[\alpha]_{578}$ = –18.6; $[\alpha]_{546}$ = –21.0; $[\alpha]_{436}$ = –34.2; $[\alpha]_{365}$ = –50.9.

**{(1*S*,2*R*)-6,6-Dimethylbicyclo[3.1.1]heptyl-2-methylene}diphenyltin Chloride {10-[(–)-*cis*-Myrtanyl]diphenyltin Chloride, 7c}:** Yield 2.4 g (5.4 mmol, 34.0%) [starting from (–)-*cis*-myrtanyl chloride (2.74 g, 15.9 mmol)]; m.p. 99–101 °C. $^1$H NMR (300.13 MHz, $CDCl_3$, 22.0 °C): $\delta$ = 0.79 (d, $^2J_{H,H}$ = 9.8 Hz, 1 H), 1.01 (s, 3 H, $CH_3$), 1.06 (s, 3 H, $CH_3$), 1.45 (m, 1 H), 1.75 (m, 2 H), 1.81/1.83 (s, 2 H), 1.89 (m, 2 H), 2.03 (m, 1 H), 2.24 (m, 1 H), 2.48 (m, 1 H), 7.36 (m, 6 H, $H_{ar}$), 7.53 (m, 4 H, $H_{ar}$) ppm. $^{13}C\{^1H\}$ NMR (75.48 MHz, $CDCl_3$, 22.0 °C): $\delta$ = 139.9 (s, Ci), 136.2 (d, $^2J_{117/119Sn,13C}$ = 48.0 Hz, $C_o$), 130.4 (d, $^4J_{117/119Sn,13C}$ = 13.1 Hz, $C_p$), 129.4 (d, $^3J_{117/119Sn,13C}$ = 58.1 Hz, $C_m$), 50.1 (s, d, $J_{117/119Sn,13C}$ = 63.9 Hz, $C_{al}$), 41.4 (s, $C_{al}$), 39.2 (s, $C_{al}$), 38.8 (s, d, $J_{117/119Sn,13C}$ = 24.7 Hz, $C_{al}$), 34.1 (s, $C_{al}$), 28.34 (s, $C_{al}$), 28.25 (d, $^1J_{117/119Sn,13C}$ = 407.6 Hz, $C_{al}$), 26.7 (s, $C_{al}$), 26.3 (s, $C_{al}$), 23.8 (s, $C_{al}$) ppm. MS (FD): *m*/*z* (%) 445 (100) $[M]^+$. $C_{22}H_{27}ClSn$ (445.62): calcd. C 59.30, H 6.11; found C 59.30, H 6.10. Optical rotation (23 °C, *c* = 0.004 in *n*-hexane): $[\alpha]_{589}$ = –1.0; $[\alpha]_{578}$ = –1.0; $[\alpha]_{546}$ = –1.5; $[\alpha]_{436}$ = –2.75; $[\alpha]_{365}$ = –5.25.

**{(1*S*,2*S*)-6,6-Dimethylbicyclo[3.1.1]heptyl-2-methylene}diphenyltin Chloride {10-[(–)-*trans*-Myrtanyl]diphenyltin Chloride, 7d}:** Yield 4.51 g (10.1 mmol, 36.5%) [starting from (–)-*trans*-myrtanyl chloride (4.78 g, 27.7 mmol)]. $^1$H NMR (300.13 MHz, $CDCl_3$, 26.9 °C): $\delta$ = 0.65 (s, 3 H, $CH_3$), 1.06 (s, 3 H, $CH_3$), 1.28 (m, 2 H), 1.32 (m, 1 H), 1.66 (m, 5 H), 1.78 (m, 1 H), 1.96 (m, 1 H), 2.39 (m, 1 H), 7.34 (m, 6 H, $H_{ar}$), 7.52 (dd, $^3J_{H,H}$ = 7.1, $^4J_{H,H}$ = 2.1, d, $^3J_{H,117/119Sn}$ = 53.8 Hz, 4 H, $H_o$) ppm. $^{13}C\{^1H\}$ NMR (75.47 MHz, $CDCl_3$, 26.9 °C): $\delta$ = 139.57 ($C_i$), 135.73 (d, $^2J_{117/119Sn,13C}$ = 47.95 Hz, $C_o$), 129.98 (d, $^4J_{117/119Sn,13C}$ = 13.0 Hz, $C_p$), 128.90 (d, $^3J_{117/119Sn,13C}$ = 57.4 Hz, $C_m$), 49.28 (s, d, $J_{117/119Sn,13C}$ = 61.0 Hz, $C_{al}$), 40.59 (s, $C_{al}$), 39.95 (s, $C_{al}$), 32.28 (s, $C_{al}$), 26.69 (s, $C_{al}$), 26.58 (s, $C_{al}$), 26.10 (s, $C_{al}$), 24.35 (s, $C_{al}$), 22.89 (s, $C_{al}$), 19.85 (s, $C_{al}$) ppm. MS (FD): *m*/*z* (%) 445 (100) $[M]^+$, 369 (2) $[(C_6H_5)(C_{10}H_{17})SnCl]^+$, 137 (2) $[C_{10}H_{17}]^+$. Optical rotation (23 °C, *c* = 0.0304 in *n*-hexane): $[\alpha]_{589}$ = –0.16; $[\alpha]_{578}$ = –0.07; $[\alpha]_{546}$ = 0.07; $[\alpha]_{436}$ = 1.78; $[\alpha]_{365}$ = 6.51.

**{3-[2-(1*R*,4*S*)-1,7,7-Trimethylbicyclo[2.2.1]hept-2-ene]phenyl}-diphenyltin Chloride {[*m*-(2-Bornyl-2-ene)phenyl]diphenyltin Chloride, 7e}:** Yield 2.50 g (4.8 mmol, 39.4%) [starting from 2-(3-chlorophenyl)bornyl-2-ene (**8e**; 3.0 g, 12.2 mmol)]. $^1$H NMR ($CDCl_3$, 269.7 MHz, 19.8 °C): $\delta$ = 0.74 (s, 3 H, $CH_3$), 0.80 (s, 3 H, $CH_3$), 1.02 (s, 3 H, $CH_3$), 1.04 (m, 1 H), 1.20 (m, 1 H), 1.58 (m, 1 H), 1.93 (m, 1 H), 2.26 (m, $^3J_{H,H3}$ = 3.5 Hz, 1 H4), 5.96 (d, $^3J_{H,H4}$ = 3.5 Hz, 1 H3), 7.40 (m, 14$H_{ar}$) ppm; the numbering scheme is the same as for **8e**. MS (FD): *m*/*z* (%) 520 (100) $[M]^+$. Optical rotation: (23 °C, *c* = 0.0824 in thf): $[\alpha]_{546}$ = –33.0; $[\alpha]_{578}$ = –28.9; $[\alpha]_{589}$ = –22.7; $[\alpha]_{633}$ = –16.5.

**Preparation of the Stannyl Triphospholes 2a–e. General Procedure:** A solution containing 1 mol of the chiral modified triorganyltin chloride [$Ph_2SnR$*Cl] (**7a**–**e**) in toluene was added to a suspension of one mol of (3,5-di-*tert*-butyl-1,2,4-triphospholyl)sodium (Na**5**) in toluene at –50 °C. After stirring and warming to room temperature overnight, all volatile components were evaporated from the reaction mixture. The resulting yellow residue was suspended in *n*-hexane and filtered to yield a clear yellow solution, which was concentrated under vacuum. Products **2a**,**b**,**d**,**e** crystallised at –30 °C as yellow solids, whereas **2c** was obtained as a yellow oil containing an impurity which could not be removed.

**2a:** Obtained from **7a** (0.42 g, 0.94 mmol) as a 63.5:36.5 mixture of *endo* and *exo* isomers. Yield 0.253 g (0.39 mmol, 42.0%). $^1$H NMR (121.49 MHz, $CDCl_3$, 25.1 °C): $\delta$ = 0.63/0.61 (s, 3 H, $CH_3$), 0.77/0.74 (s, 3 H, $CH_3$), 1.13/1.08 (s, 3 H, $CH_3$), 1.51/1.46 [br., 2×18 H, $C(CH_3)_3$], 2.58–0.50 (m, 8 H, CH, $CH_2$), 7.67–6.96 (m, 10 H, $H_{ar}$) ppm. $^{13}C\{^1H\}$ NMR (100.40 MHz, $C_6D_5CD_3$, 21.7 °C): $\delta$ = 219.18/219.68 [2×d pseudo t, $^1J_{P,C}$ = 35.9/35.3, $\Sigma(^1J_{P,C} + {}^2J_{P,C})$ = 65.3/65.2 Hz, $C_{ring}$), 41.25/41.19 [2×d pseudo t, $^2J_{P,C}$ = 19.8/19.9, $\Sigma(^2J_{P,C} + {}^3J_{P,C})$ = 5.7/5.8 Hz, $C(CH_3)$], 34.97 [d pseudo t, $^3J_{P,C}$ = 10.7, $\Sigma(^3J_{P,C} + {}^4J_{P,C})$ = 5.7 Hz, $C(CH_3)$], 141.15/139.60 and 139.93/139.48 (t, $^2J_{P,C}$ = 3.7/5.7 and 4.1/5.8 Hz, 2×2 $C_i$), 135.60 (m, $C_o$), 127.50–124.00* (m, $C_p$/$C_m$) ppm. Two sets of signals for aliphatic carbon atoms: $\delta$ = 49.13, 48.73, 48.00, 47.38, 46.70, 46.51, 45.81, 45.42, 40.24, 40.17, 36.96, 34.11, 26.99, 26.52, 20.35–17.14* ppm (s, 6×$CH_3$); * denotes signals that are partially superimposed by solvent signals. $^{31}P\{^1H\}$ NMR (161.70 MHz, $C_6D_5CD_3$, 22.9 °C): *endo* isomer: $\delta$ = 317.13 (t, $^2J_{P,P}$ = 37.2 + d, $^3J_{31P,117/119Sn}$ = 35.6 Hz, 1 P, P3), 160.95 (d, $^2J_{P,P}$ = 37.2 + d, $J_{31P,117/119Sn}$ = 378.9 Hz, 2 P,

  

P1+P2) ppm; *exo* isomer: $\delta$ = 315.75 (t, $^2J_{P,P}$ = 40.4 + d, $^3J_{^{31}P,^{117/119}Sn}$ = 37.2 Hz, 1 P, P3′), 162.21 (d, $^2J_{P,P}$ = 40.4 + d, $J_{^{31}P,^{117/119}Sn}$ = 386.7 Hz, 2 P, P1′ + P2′) ppm. MS (FD): *m/z* (%) 641 (100) $[M]^+$, 411 (1) $[(C_{10}H_{17})(C_6H_5)_2Sn]^+$, 231 (1) $[(C_2P_3{}^tBu_2)_2Sn]^+$, 137 (3) $[(C_{10}H_{17})]^+$. No clear melting behaviour or correct analytical results could be obtained due to the solvent content of the crystalline material.

**2b:** Obtained from **7b** (1.94 g, 4.3 mmol) as a mixture of two epimers. Yield 2.06 g (80.2%). $^1$H NMR (269.72 MHz, $CDCl_3$, 25.1 °C): $\delta$ = 0.61 (d, $J_{H,H}$ = 6.7 Hz, 3 H, $CH_3$), 0.66 (d, $J_{H,H}$ = 6.7 Hz, 3 H, $CH_3$), 0.72 (d, $J_{H,H}$ = 6.6 Hz, 6 H, 2×$CH_3$), 0.75 (3 H, $CH_3$), 0.88 (d, $J_{H,H}$ = 6.6 Hz, 3 H, $CH_3$), 0.76–2.33 (m, 2×9 H), 1.39/1.36 (2 s, 2×18 H, C(C$H_3$)$_3$], 3.21 (br. d, $^2J_{H,^{117/119}Sn} \approx$ 59 Hz, 2×1 H), 7.27 (m, 6 H, $H_{m/p}$), 7.39 (m, $^3J_{H,^{117/119}Sn}$ = 49.9 Hz, 4 H, $H_o$) ppm. $^{13}$C{$^1$H} NMR (67.83 MHz, $CDCl_3$, 25.1 °C): $\delta$ = 221.45/220.15 [2×d pseudo t, $^1J_{P,C}$ = 36.0/36.0, $\Sigma(^1J_{P,C} + {}^2J_{P,C})$ = 65.3/63.4 Hz, $C_{ring}$], 42.44/42.34 [2×d pseudo t, $^2J_{P,C}$ = 20.5/20.5, $\Sigma(^2J_{P,C} + {}^3J_{P,C})$ = 6.2/5.6 Hz, *C*($CH_3$)], 36.12/36.11 [2×d pseudo t, $^3J_{P,C}$ = 10.6/11.2, $\Sigma(^3J_{P,C} + {}^4J_{P,C})$ = 5.0/5.6 Hz, C(*C*$H_3$)], 140.88/140.53/138.69/138.60 (t, $^2J_{P,C}$ = 4.3/3.7/4.4/7.5 Hz, 2×$C_i$/$C_{i'}$), 135.94/135.71/135.66/135.55 (s, 2×$C_o$/$C_{o'}$), 127.46 (m, 2×$C_m$/$C_{m'}$/$C_p$/$C_{p'}$); 2×10 signals of the epimeric menthyl substituents: 49.28 (s, $C_{al}$), 46.93 (s, $C_{al}$), 45.71 (s, $C_{al}$), 45.05 (s, $C_{al}$), 43.75 (s, $C_{al}$), 40.64 (s, $C_{al}$), 40.12 (s, $C_{al}$), 49.32 (s, $C_{al}$), 38.46 (s, $C_{al}$), 38.19 (s, $C_{al}$), 33.00 (s, $C_{al}$), 32.12 (s, $C_{al}$), 28.49 (s, $C_{al}$), 25.88 (s, $C_{al}$), 21.72 (s, $C_{al}$), 21.56 (s, $C_{al}$), 21.38 (s, $C_{al}$), 20.80 (s, $C_{al}$), 19.96 (s, $C_{al}$), 15.14 (s, $C_{al}$) ppm. $^{31}$P{$^1$H} NMR (121.49 MHz, $CDCl_3$, 25.1 °C, 2 sets of signals of the $AB_2$ spin system): $\delta$ = 319.73 (t, $^2J_{P,P}$ = 38.8 + d, $^3J_{^{31}P,^{117/119}Sn}$ = 40.7 Hz, 1 P, P4), 162.16 (d, $^2J_{P,P}$ = 38.8 + d, $J_{^{31}P,^{117/119}Sn}$ = 377.3 Hz, 2 P, P1 + P2), 315.32 (t, $^2J_{P,P}$ = 38.8 + d, $^3J_{^{31}P,^{117/119}Sn}$ = 37.0 Hz, 1 P, P4′), 163.15 (d, $^2J_{P,P}$ = 38.8 + d, $J_{^{31}P,^{117/119}Sn}$ = 381.0 Hz, 2 P, P1′ + P2′) ppm. MS (FD): *m/z* (%) 643 (100) $[M]^+$, 139 (5) $[C_{10}H_{19}]^+$. $C_{32}H_{47}P_3Sn$ (643.35): calcd. C 59.74, H 7.36; found C 60.66, H 8.28. Optical rotation (24 °C, *c* = 0.026 in *n*-hexane): $[\alpha]_{546}$ = 17.5; $[\alpha]_{578}$ = 12.8; $[\alpha]_{589}$ = 11.6.

**2c:** Obtained as yellow oil containing about 8.5% of a known $P_6C_4{}^tBu_4H_2$ cage,[43] which could not be removed, from **7c** (0.79 g, 1.77 mmol). Yield 1.02 g (1.59 mmol, 90%). $^1$H NMR (300.13 MHz, $CDCl_3$, 25.0 °C): $\delta$ = 0.66 (d, $^2J_{H,H}$ = 9.4 Hz, 2 H, $CH_2$), 0.96 (s, 3 H, $CH_3$), 0.99 (s, 3 H, $CH_3$), 1.41 [s, 18 H, 2×C($CH_3$)$_3$], 1.72 (m, 7 H), 2.20 (m, 2 H), 7.25 (m, 6 H, $H_{ar}$), 7.31 (m, 4 H, $H_{ar}$) ppm. $^{13}$C{$^1$H} NMR (75.47 MHz, $CDCl_3$, 25.0 °C): $\delta$ = 222.0 [d pseudo t, $J_{P,C}$ = 36.3, $\Sigma(J_{P,C} + {}^2J_{P,C})$ = 64.7 Hz, $C_{ring}$], 42.83 [d pseudo t, $^2J_{P,C}$ = 20.3, $\Sigma(^2J_{P,C} + {}^3J_{P,C})$ = 5.8 Hz, *C*($CH_3$)], 36.49 [d pseudo t, $^3J_{P,C}$ = 10.9, $\Sigma(^3J_{P,C} + {}^4J_{P,C})$ = 5.8 Hz, C(*C*$H_3$)], 140.63/140.45 (s, $^2J_{P,C}$ = 5.1 Hz, $C_i$), 137.03/136.97 (s, $^2J_{^{117/119}Sn,^{13}C}$ = 40.0 Hz, $C_o$), 129.67 (s, $^4J_{^{117/119}Sn,^{13}C}$ = 11.6 Hz, $C_p$), 129.02 (s, $^3J_{^{117/119}Sn,^{13}C}$ = 52.4 Hz, $C_m$), 50.0 (s, $J_{^{117/119}Sn,^{13}C}$ = 54.5 Hz), 41.53, 39.68 (s, $J_{^{117/119}Sn,^{13}C}$ = 24.0 Hz), 39.17, 34.27, 28.41, 28.20, 26.84, 26.46, 23.84 ppm. $^{31}$P{$^1$H} NMR (121.49 MHz, $CDCl_3$, 25.1 °C): $\delta$ = 319.30 (t, $^2J_{P,P}$ = 37.9 + d, $^3J_{^{31}P,^{117/119}Sn}$ = 51.2 Hz, 1 P, P3), 162.0 (d, $^3J_{P,P}$ = 37.9 + d, $J_{^{117/119}Sn,^{31}P}$ = 356.4 Hz, 2 P, P1 + P2) ppm. MS (FD): *m/z* (%) 641 (100) $[M]^+$, 410 (1) $[(C_6H_5)_2(C_{10}H_{17})Sn]^+$, 231 (2) $[C_2P_3{}^tBu_2]^+$. Optical rotation (23 °C, *c* = 0.0026 in *n*-hexane): $[\alpha]_{589}$ = –10.0; $[\alpha]_{578}$ = –10.4; $[\alpha]_{546}$ = –11.2.

**2d:** Synthesised from **7d** (0.62 g, 1.4 mmol). Yield 0.65 g (1.0 mmol, 72.3%) $^1$H NMR (300.13 MHz, $CD_2Cl_2$, 26.9 °C): $\delta$ = 0.52 (s, 3 H, $CH_3$), 0.97 (s, 3 H, $CH_3$), 0.99–1.59 (m, 8 H, $H_{al}$ + $CH_2$), 1.40 [s, 18 H, C(C$H_3$)$_3$], 1.72 (m, 1 H), 1.91 (m, 1 H), 2.18 (m, 1 H), 6.95–7.10 (m, 6 H, $H_{ar}$), 7.37 (ddd, $^3J_{H,H}$ = 7.7, $^4J_{H,H}$ = 2.4, $^4J_{H,H}$ = 1.7 + d, $^3J_{^{117/119}Sn,H}$ = 49.9 Hz, 4 H, $H_{ar}$) ppm. $^{13}$C{$^1$H} NMR (75.47 MHz, $CD_2Cl_2$, 26.9 °C): $\delta$ = 222.60 [d pseudo t, $J_{P,C}$ = 35.8, $\Sigma(J_{P,C} + {}^2J_{P,C})$ = 64.7 Hz, $C_{ring}$], 43.30 [d pseudo t, $^2J_{P,C}$ = 20.8, $\Sigma(^2J_{P,C} + {}^3J_{P,C})$ = 5.8 Hz, *C*($CH_3$)], 36.37 [d pseudo t, $^3J_{P,C}$ = 10.4, $\Sigma(^3J_{P,C} + {}^4J_{P,C})$ = 5.8 Hz, C(*C*$H_3$)], 141.17 (d, $J_{^{117/119}Sn,^{13}C}$ = 469.3 + d, $^2J_{P,C}$ = 4.6 Hz, $C_i$), 137.55 (d, $^2J_{^{117/119}Sn,^{13}C}$ = 40.4 Hz, $C_o$), 129.54 (d, $^3J_{^{117/119}Sn,^{13}C}$ = 52.0 Hz, $C_m$), 130.23 (d, $^4J_{^{117/119}Sn,^{13}C}$ = 9.3 Hz, $C_p$), 50.12, 41.64, 40.75, 34.00, 27.48, 27.36, 26.52, 25.45, 23.75, 20.53 ppm. $^{31}$P{$^1$H} NMR (121.49 MHz, $CD_2Cl_2$, 25.1 °C): $\delta$ = 318.90 (t, $^2J_{P,P}$ = 38.8 + d, $^3J_{^{31}P,^{117/119}Sn}$ = 51.2 Hz, 1 P, P4), 162.25 (d, $^3J_{P,P}$ = 38.8 + d, $J_{^{117/119}Sn,^{31}P}$ = 358.7 Hz, 2 P, P1 + P2) ppm. MS (FD): *m/z* (%) 641 (100) $[M]^+$, 410 (22) $[(C_6H_5)_2(C_{10}H_{17})Sn]^+$, 231 (15) $[C_2P_3{}^tBu_2]^+$, 137 (2) $[C_{10}H_{17}]^+$. M.p. 86–88 °C. $C_{32}H_{45}P_3Sn$ (641.34): calcd. C 59.93, H 7.07; found C 59.34, H 7.54. Optical rotation (23 °C, *c* = 0.0024 in *n*-hexane): $[\alpha]_{589}$ = 1.25; $[\alpha]_{578}$ = –16.67; $[\alpha]_{546}$ = 4.17.

**2e:** Synthesised from **7e** (2.03 g, 3.9 mmol). Yield 1.71 g (2.4 mmol, 63.4%). $^1$H NMR (300.13 MHz, $CDCl_3$, 26.9 °C): $\delta$ = 0.73 (s, 3 H, $CH_3$), 0.79 (s, 3 H, $CH_3$), 0.98 (s, 3 H, $CH_3$), 1.03 (m, 1 H), 1.19 (m, 1 H), 1.38 [s, 18 H, C(C$H_3$)$_3$], 1.56 (m, 1 H), 1.85 (m, 1 H), 2.30 (m, $^3J_{H,H3}$ = 3.3 Hz, 1 H, H4), 5.89 (d, $^3J_{H,H4}$ = 3.3 Hz, 1 H, H3), 7.31 (m, 14 H, $H_{ar}$) ppm. $^{13}$C{$^1$H} NMR (75.47 MHz, $CDCl_3$, 26.9 °C): $\delta$ = 222.76 [d pseudo t, $J_{P,C}$ = 37.0, $\Sigma(J_{P,C} + {}^2J_{P,C})$ = 64.9 Hz, $C_{Ring}$], 42.96 [d pseudo t, $^2J_{P,C}$ = 19.6, $\Sigma(^2J_{P,C} + {}^3J_{P,C})$ = 5.8 Hz, *C*($CH_3$)], 36.37 [d pseudo t, $^3J_{P,C}$ = 10.9, $\Sigma(^3J_{P,C} + {}^4J_{P,C})$ = 5.8 Hz, C(*C*$H_3$)], 149.90, 139.30, 139.19, 138.33 (d, $J_{^{117/119}Sn,^{13}C}$ = 8.7 Hz, $C_{ar/olef}$), 137.18 (d, $^2J_{^{117/119}Sn,^{13}C}$ = 40.7 Hz, $C_o$), 135.27, 134.99, 132.68, 129.93 (d, $^4J_{^{117/119}Sn,^{13}C}$ = 13.1 Hz, $C_p$), 129.11, 128.74, 128.23, 57.52, 55.32, 52.07, 32.80, 26.08, 20.14, 20.06, 13.06 ppm. $^{31}$P{$^1$H} NMR (121.49 MHz, $CDCl_3$, 25.1 °C): $\delta$ = 325.05 (t, $^2J_{P,P}$ = 38.8 + d, $^3J_{^{31}P,^{117/119}Sn}$ = 66.6 Hz, 1 P, P4), 159.24 (d, $^2J_{P,P}$ = 38.8 + d, $J_{^{31}P,^{117/119}Sn}$ = 351.4 Hz, 2 P, P1 + P2) ppm. MS (FD): *m/z* (%) 715 (100) $[M]^+$, 212 (34) $[C_6H_5 - C_{10}H_{15}]^+$. M.p. 86–88 °C. Optical rotation (23 °C, *c* = 0.0121 in *n*-hexane): $[\alpha]_{589}$ = –52.3; $[\alpha]_{578}$ = –55.0; $[\alpha]_{546}$ = –64.1.

**Crystal Structure Determinations:** Intensity data for **2a** and **2b** were collected with a Siemens P4 diffractometer ($\omega$ scan technique, 4.0°/min), whereas those for (*R*)-**7b** were collected with a Nicolet R3m/V diffractometer ($\omega$ scan technique, 8.0°/min) and those for **2d** and **7c** with a Bruker–Nonius KappaCCD diffractometer ($\phi$ and $\omega$ rotations). Mo-$K_\alpha$ radiation (graphite monochromator, $\lambda$ = 0.71073 Å) was used for all data collections and data were corrected for Lorentz and polarisation effects. Absorption effects were taken into account for **2a**, **2b** and (*R*)-**7b** by using a semi-empirical method based on Psi-scans.[44] A numerical absorption method was applied[45] for **2d** and a semi-empirical method based on multiple scans (SADABS, Bruker-AXS, 2002)[46] was used for **7c**. All structures were solved by direct methodsand refined by full-matrix least-squares procedures against $F^2$ with all reflections using SHELXTL-NT 6.12 (Bruker AXS, 2002).[47] All non-hydrogen atoms were refined anisotropically. The hydrogen atoms were placed in optimised positions with an isotropic displacement parameter corresponding to 1.2- or 1.5-times the equivalent isotropic displacement parameter of their parent carbon atoms. The crystal structure of **2a** contains 1.5 molecules of toluene in the asymmetric unit. The half molecule of toluene is disordered over a crystallographic inversion centre and was refined using SIMU restraints. Crystal data and experimental details are listed in Table 4.

CCDC-660896 (for **2a**; originally deposited as **6a**), -660897 (for **2b**; deposited as **6b**), -660898 (for **2d**; deposited as **6d**), -660899 (for **7c**; deposited as **8c**) and -660900 [for (*R*)-**7b**; deposited as **8d**) contain the supplementary crystallographic data for this paper. These data can be obtained free of charge from The Cambridge Crystallographic Data Centre via www.ccdc.cam.ac.uk/data_request/cif.

  

Table 4. Experimental data from X-ray diffraction studies.

| | **2a** | **2b** | **2d** | **7b** | **7c** |
|---|---|---|---|---|---|
| Formula | $C_{42.5}H_{57}P_3Sn$ | $C_{32}H_{47}P_3Sn$ | $C_{32}H_{45}P_3Sn$ | $C_{22}H_{29}ClSn$ | $C_{22}H_{27}ClSn$ |
| Crystal size [mm] | $0.60\times0.50\times0.10$ | $0.60\times0.55\times0.42$ | $0.30\times0.28\times0.21$ | $0.66\times0.22\times0.18$ | $0.18\times0.13\times0.05$ |
| Crystal system | triclinic | triclinic | monoclinic | monoclinic | orthorhombic |
| Space group | $P\bar{1}$ | $P1$ | $P2_1$ | $P2_1$ | $P2_12_12_1$ |
| $a$ [pm] | 1105.7(2) | 979.9(1) | 1018.32(2) | 1892.6(6) | 999.15(6) |
| $b$ [pm] | 1365.7(2) | 1322.8(2) | 3312.51(5) | 607.3(2) | 1068.97(4) |
| $c$ [pm] | 1452.7(2) | 1374.9(2) | 1055.94(2) | 1934.3(7) | 1875.4(1) |
| $\alpha$ [°] | 71.67(1) | 75.56(1) | 90 | 90 | 90 |
| $\beta$ [°] | 88.39(1) | 75.51(1) | 118.230(2) | 95.39(3) | 90 |
| $\gamma$ [°] | 82.10(1) | 78.78(1) | 90 | 90 | 90 |
| $V$ [nm$^3$] | 2.0623(6) | 1.6543(4) | 3.1382(1) | 2.213(2) | 2.0030(2) |
| $Z$ | 2 | 2 | 4 | 4 | 4 |
| $M_r$ | 779.52 | 643.35 | 641.34 | 447.61 | 445.62 |
| $\mu$ [mm$^{-1}$] | 0.763 | 0.935 | 0.986 | 1.276 | 1.409 |
| $T_{min}/T_{max}$ | 0.714/0.929 | 0.621/0.677 | 0.638/0.823 | 0.678/0.795 | 0.775/0.930 |
| $\rho$ [g cm$^{-3}$] | 1.255 | 1.291 | 1.357 | 1.343 | 1.478 |
| $F$(000) | 814 | 668 | 1328 | 912 | 904 |
| $T$ (data coll.) [K] | 200 (2) | 210 (2) | 100 (2) | 298 (2) | 100 (2) |
| $2\Theta$ range [°] | 4.5–54.0 | 4.7–55.8 | 7.6–55.8 | 5.8–50.1 | 7.0–55.8 |
| $hkl$ range | –13/9 –16/16 –18/18 | –12/7 –17/16 –18/17 | –13/13 –42/43 –13/13 | –22/22 –7/7 –1/23 | –12/12 –11/13 –22/24 |
| Reflections measured | 14632 | 10615 | 56778 | 7772 | 23625 |
| Reflections unique | 8837 | 10554 | 14580 | 7116 | 4691 |
| Reflections observed [$I\geq4\sigma(I)$] | 7262 | 9968 | 13558 | 3744 | 4446 |
| Parameters refined | 436 | 669 | 665 | 433 | 219 |
| GooF (all data) | 1.017 | 1.077 | 1.041 | 0.961 | 0.997 |
| *R1* (obsd. reflections) | 0.0415 | 0.0279 | 0.0318 | 0.0591 | 0.0166 |
| *wR2* (all data) | 0.1142 | 0.0740 | 0.0741 | 0.1630 | 0.0333 |
| Absolute structure parameter | – | 0.015(16) | 0.009(11) | 0.16(10) | –0.028(11) |

**Supporting Information** (see also the footnote on the first page of this article): Details of the theoretical calculations (4 pages, complete set of basis calculation data for ground states **9a**–**c** and transition states $\mathbf{T_i}$ and $\mathbf{T_s}$).

## Acknowledgments

This work was supported by the Deutsche Forschungsgemeinschaft (DFG). We thank Drs. M. Moll and A. Zahl for measuring the variable-temperature NMR spectra.

[1] J. M. O'Connor, C. P. Casey, *Chem. Rev.* **1987**, *87*, 307.
[2] A. Davison, P. E. Rakita, *Inorg. Chem.* **1970**, *9*, 289; W. Kläui, H. Werner, *Helv. Chim. Acta* **1976**, *59*, 844.
[3] S. T. Abu-Orabi, P. Jutzi, *J. Organomet. Chem.* **1987**, *329*, 169.
[4] C. Charrier, H. Bonnard, G. de Lauzon, F. Mathey, *J. Am. Chem. Soc.* **1983**, *105*, 6871; S. Holand, F. Mathey, J. Fischer, *Polyhedron* **1986**, *5*, 1413.
[5] M. L. Sierra, N. Maigrot, C. Charrier, L. Ricard, F. Mathey, *Organometallics* **1991**, *10*, 2835; F. G. N. Cloke, P. B. Hitchcock, J. F. Nixon, L. Nyulászi, T. Kárpáti, *J. Organomet. Chem.* **2005**, *690*, 3983.
[6] D. A. Pantazis, J. E. McGrady, J. M. Lynam, C. A. Russell, M. Green, *Dalton Trans.* **2004**, 2080.
[7] A. Elvers, F. W. Heinemann, B. Wrackmeyer, U. Zenneck, *Chem. Eur. J.* **1999**, *5*, 3143; A. Elvers, F. W. Heinemann, S. Kummer, B. Wrackmeyer, M. Zeller, U. Zenneck, *Phosphorus Sulfur Silicon Relat. Elem.* **1999**, *144–146*, 725.
[8] K. Forissier, L. Ricard, D. Carmichael, F. Mathey, *Chem. Commun.* **1999**, 1273.
[9] F. G. N. Cloke, K. R. Flower, C. Jones, R. M. Matos, J. F. Nixon, *J. Organomet. Chem.* **1995**, *487*, C21.
[10] K. M. Pietrusiewicz, M. Zablocka, *Chem. Rev.* **1984**, *94*, 1375; G. Hoge, *J. Am. Chem. Soc.* **2004**, *126*, 9920.
[11] Z. Csók, G. Keglevich, G. Petöcz, L. Kollár, *Inorg. Chem.* **1999**, *38*, 831; V. Mouriès, F. Mercier, L. Ricard, F. Mathey, *Eur. J. Org. Chem.* **1998**, 2683; J. Grundy, B. Donnadieu, F. Mathey, *J. Am. Chem. Soc.* **2006**, *128*, 7716; P. Rosa, L. Ricard, F. Mathey, P. Le Floch, *Chem. Commun.* **1999**, 537; M. Westerhausen, M. H. Digeser, H. Nöth, W. Ponikwar, T. Seifert, K. Polborn, *Inorg. Chem.* **1999**, *38*, 3207; J. Holz, A. Monsees, R. Kadyrov, A. Börner, *Synlett* **2007**, *4*, 599; R. Streubel, U. Schiemann, P. G. Jones, J. Grunenberg, H.-M. Schiebel, D. Gudat, *Angew. Chem. Int. Ed.* **2001**, *40*, 2471; M. Sauthier, F. Leca, L. Toupet, R. Réau, *Organometallics* **2002**, *21*, 1591.
[12] S. Gladiali, A. Dore, D. Fabbri, O. De Lucchi, G. Vaile, *J. Org. Chem.* **1994**, *59*, 6363.
[13] R. H. Bowman, K. Mislow, *J. Am. Chem. Soc.* **1972**, *94*, 2862.
[14] F. W. Heinemann, H. Pritzkow, M. Zeller, U. Zenneck, *Organometallics* **2000**, *19*, 4283.
[15] R. Bartsch, D. Carmichael, P. B. Hitchcock, M. F. Meidine, J. F. Nixon, G. J. D. Sillett, *J. Chem. Soc., Chem. Commun.* **1988**, 1615; J. F. Nixon, G. J. D. Sillett, *J. Organomet. Chem.* **1993**, *461*, 237.
[16] F. W. Heinemann, M. Zeller, U. Zenneck, *Organometallics* **2004**, *23*, 1689.
[17] D. A. Atwood, L. Ricard, F. Mathey, P. Le Floch, *Inorg. Chem.* **1993**, *32*, 1527.
[18] M. Hofmann, F. W. Heinemann, U. Zenneck, *J. Organomet. Chem.* **2002**, *643–644*, 357; M. M. Al-Ktaifani, P. B. Hitchcock, J. F. Nixon, *J. Organomet. Chem.* **2003**, *665*, 101.
[19] T. K. Hollis, Y. Joun Ahn, F. S. Tham, *Chem. Commun.* **2002**, 2996; T. K. Hollis, Y. Joun Ahn, F. S. Tham, *Organometallics* **2003**, *22*, 1432; Y. Joun Ahn, R. J. Rubio, T. K. Hollis, F. S. Tham, B. Donnadieu, *Organometallics* **2006**, *25*, 1079; T. K. Hollis, L.-S. Wang, F. Tham, *J. Am. Chem. Soc.* **2000**, *122*, 11737; S. Bellemin-Laponnaz, M. M. C. Lo, T. H. Peterson, J. M. Allen, G. C. Fu, *Organometallics* **2001**, *20*, 3453.

  

[20] F. G. N. Cloke, P. B. Hitchcock, P. Hunnable, J. F. Nixon, L. Nyulászi, E. Nieke, V. Thelen, *Angew. Chem. Int. Ed.* **1998**, *37*, 1083.
[21] F. E. Hahn, L. Wittenbacher, D. Le Van, R. Fröhlich, B. Wibbeling, *Angew. Chem. Int. Ed.* **2000**, *39*, 2307; S. B. Clendenning, P. B. Hitchcock, J. F. Nixon, L. Nyulászi, *Chem. Commun.* **2000**, 1305.
[22] G. Becker, G. Gresser, W. Uhl, *Z. Naturforsch. Teil B* **1981**, *36*, 16; G. Becker, W. Becker, R. Knebl, H. Schmidt, U. Weeber, M. Westerhausen, *Nova Acta Leopold.* **1985**, *59*, 55.
[23] R. Bartsch, J. F. Nixon, *Polyhedron* **1989**, *8*, 2407.
[24] C. Fish, M. Green, J. C. Jeffery, R. J. Kilby, J. M. Lynam, C. A. Russell, C. E. Willans, *Organometallics* **2005**, *24*, 5789.
[25] H. C. Brown, K.-T. Liu, *J. Am. Chem. Soc.* **1975**, *11*, 600.
[26] R. J. Abraham, A. P. Barlow, A. E. Rowan, *Magn. Reson. Chem.* **1989**, *27*, 1074.
[27] A. Marinetti, F. X. Buzin, L. Ricard, *J. Org. Chem.* **1997**, *62*, 297.
[28] M. Hofmann, Diploma Thesis, University of Erlangen-Nürnberg, **1998**.
[29] R. D. Rieke, Organic Syntheses, Topics in Current Chemistry, *Use of Activated Metals in Organic and Organometallic Synthesis*, Springer-Verlag Berlin Heidelberg New York, **1975**, pp. 3.
[30] H. Schumann, G. Rodewald, U. Rodewald, J. L. Lefferts, J. J. Zimmermann, *J. Organomet. Chem.* **1980**, *187*, 305.
[31] R. Krishnamurti, H. G. Kuivila, *J. Org. Chem.* **1986**, *51*, 4947; M. Helliwell, E. J. Thomas, L. A. Townsend, *J. Chem. Soc. Perkin Trans. 1* **2002**, 1286; E. A. Hill, *J. Org. Chem.* **1966**, *31*, 20.
[32] M. Tanaka, I. Ogata, *Bull. Chem. Soc. Jpn.* **1975**, *48*, 1094; H. Schumann, B. C. Wassermann, *J. Organomet. Chem.* **1989**, *365*, C1; H. Schumann, B. C. Wassermann, F. E. Hahn, *Organometallics* **1992**, *11*, 2803; J. C. Podestá, A. B. Chopa, G. E. Radivoy, C. A. Vitale, *J. Organomet. Chem.* **1995**, *494*, 11; C. Lucas, C. C. Santini, M. Prinz, M.-A. Cordonnier, J.-M. Basset, M.-F. Connil, B. Jousseaume, *J. Organomet. Chem.* **1996**, *520*, 101.
[33] M. B. Faraoni, A. D. Ayala, V. Vetere, M. L. Casella, O. A. Ferretti, J. C. Podestá, *Appl. Organomet. Chem.* **2005**, *19*, 465; J. Beckmann, D. Dakternieks, M. Dräger, A. Duthie, *Angew. Chem. Int. Ed.* **2006**, *45*, 6509.
[34] H. D. Flack, *Acta Crystallogr., Sect. A* **1983**, *39*, 876.
[35] M. Eisen, P. Weitz, S. Shteizer, J. Blum, H. Schumann, B. Gorella, F. H. Görlitz, *Inorg. Chim. Acta* **1991**, *188*, 167.
[36] P. G. Jones, K. Schmidt-Bäse, M. R. Edwards, A. J. Kirby, *Acta Crystallogr., Sect. C* **1992**, *48*, 826; H. Adams, N. A. Bailey, D. N. Jones, M. C. Aversa, P. Bonaccorsi, P. Giannetto, *Acta Crystallogr., Sect. C* **1995**, *51*, 1357.
[37] M. J. Frisch, G. W. Trucks, H. B. Schlegel, G. E. Scuseria, M. A. Robb, J. R. Cheeseman, J. A. Montgomery Jr, T. Vreven, K. N. Kudin, J. C. Burant, J. M. Millam, S. S. Iyengar, J. Tomasi, V. Barone, B. Mennucci, M. Cossi, G. Scalmani, N. Rega, G. A. Petersson, H. Nakatsuji, M. Hada, M. Ehara, K. Toyota, R. Fukuda, J. Hasegawa, M. Ishida, T. Nakajima, Y. Honda, O. Kitao, H. Nakai, M. Klene, X. Li, J. E. Knox, H. P. Hratchian, J. B. Cross, C. Adamo, J. Jaramillo, R. Gomperts, R. E. Stratmann, O. Yazyev, A. J. Austin, R. Cammi, C. Pomelli, J. W. Ochterski, P. Y. Ayala, K. Morokuma, G. A. Voth, P. Salvador, J. J. Dannenberg, V. G. Zakrzewski, S. Dapprich, A. D. Daniels, M. C. Strain, O. Farkas, D. K. Malick, A. D. Rabuck, K. Raghavachari, J. B. Foresman, J. V. Ortiz, Q. Cui, A. G. Baboul, S. Clifford, J. Cioslowski, B. B. Stefanov, G. Liu, A. Liashenko, P. Piskorz, I. Komaromi, R. L. Martin, D. J. Fox, T. Keith, M. A. Al-Laham, C. Y. Peng, A. Nanayakkara, M. Challacombe, P. M. W. Gill, B. Johnson, W. Chen, M. W. Wong, C. Gonzalez, and J. A. Pople, *Gaussian*, Inc., Pittsburgh PA, **2003**.
[38] T. H. Dunning Jr, and P. J. Hay, in *Modern Theoretical Chemistry* (Ed.: H. F. Schaefer III), vol. 3, Plenum, New York, **1976**, 1.
[39] M. J. Frisch, J. A. Pople, J. S. Binkley, *J. Chem. Phys.* **1984**, *80*, 3265.
[40] A. D. Becke, *J. Chem. Phys.***1993**, *98*, 5648; A. D. Becke, in *The Challenge of d- and f-electrons: Theory and Computation* (Eds.: D. R. Salahub, M. C. Zerner), American Chemical Society, Washington, DC, **1989**, 165; S. H. Vosko, L. Wilk, M. Nusait, *Can. J. Phys.* **1980**, *58*, 1200; C. Lee, W. Yang, R. G. Parr, *Phys. Rev. B* **1988**, *37*, 785.
[41] J. Cizek, *Adv. Chem. Phys.* **1969**, *14*, 35; G. D. Purvis, R. J. Bartlett, *J. Chem. Phys.* **1982**, *76*, 1910; G. E. Scuseria, C. L. Janssen, H. F. Schaefer III, *J. Chem. Phys.* **1988**, *89*, 7382; G. E. Scuseria, H. F. Schaefer III, *J. Chem. Phys.* **1989**, *90*, 3700.
[42] J. A. Pople, M. Head-Gordon, K. Raghavachari, *J. Chem. Phys.* **1987**, *87*, 5968.
[43] R. Bartsch, P. B. Hitchcock, J. F. Nixon, *J. Chem. Soc., Chem. Commun.* **1989**, 1046.
[44] A. C. T. North, D. C. Phillips, F. S. Mathews, *Acta Crystallogr., Sect. A* **1968**, *24*, 351.
[45] P. Coppens, in *Crystallographic Computing* (Ed.: F. R. Ahmed, S. R. Hall, C. P. Huber), Munksgaard, Copenhagen, **1970**, pp. 255–270.
[46] *SADABS 2.08*, Bruker AXS, Inc., Madison, WI, U. S. A., **2002**.
[47] *SHELXTL NT 6.12*, Bruker AXS, Inc., Madison, WI, U. S. A., **2002**.

Received: December 7, 2007
Published Online: April 1, 2008

  